Environment International 179 (2023) 108169

Contents lists available at ScienceDirect

Environment International

journal homepage: www.elsevier.com/locate/envint

Full length article

Systems toxicology of complex wood combustion aerosol reveals gaseous carbonyl compounds as critical constituents

Marco Dilger [a,b], Olivier Armant [b,c], Larissa Ramme [a,b], Sonja Mülhopt [a,d], Sean C. Sapcariu [a,e], Christoph Schlager [a,d], Elena Dilger [f], Ahmed Reda [a,g,h], Jürgen Orasche [a,g,h], Jürgen Schnelle-Kreis [a,h], Thomas M. Conlon [i], Ali Önder Yildirim [a,i], Andrea Hartwig [f], Ralf Zimmermann [a,g,h], Karsten Hiller [a,e], Silvia Diabaté [a,b], Hanns-Rudolf Paur [a,d], Carsten Weiss [b,*]

[a] HICE – Helmholtz Virtual Institute of Complex Molecular Systems in Environmental Health – Aerosols and Health, Germany[1]
[b] Institute of Biological and Chemical Systems, Biological Information Processing, Karlsruhe Institute of Technology, Campus North, Eggenstein-Leopoldshafen, Germany
[c] Institut de Radioprotection et de Sureté Nucléaire (IRSN), PSE-ENV/SRTE/LECO, Cadarache, Saint-Paul-lez-Durance 13115, France
[d] Institute for Technical Chemistry, Karlsruhe Institute of Technology, Campus North, Eggenstein-Leopoldshafen, Germany
[e] Luxembourg Centre for Systems Biomedicine, University of Luxembourg, L-4362 Esch-Belval, Luxembourg
[f] Institute of Applied Biosciences, Department of Food Chemistry and Toxicology, Karlsruhe Institute of Technology (KIT), Karlsruhe, Germany
[g] Joint Mass Spectrometry Centre, Chair of Analytical Chemistry, Institute of Chemistry, University Rostock, Germany
[h] Joint Mass Spectrometry Centre, CMA – Comprehensive Molecular Analytics, Helmholtz Zentrum München, Neuherberg, Germany
[i] Institute of Lung Health and Immunity (LHI), Comprehensive Pneumology Center (CPC), Helmholtz Zentrum München, Member of the German Center for Lung Research (DZL), Neuherberg, Germany

ARTICLE INFO

Handling Editor: Hanna Boogaard

Keywords:
Air pollution
Wood smoke
Systems toxicology
Lung cells
Air–liquid interface
Carbonyl compounds

ABSTRACT

Epidemiological studies identified air pollution as one of the prime causes for human morbidity and mortality, due to harmful effects mainly on the cardiovascular and respiratory systems. Damage to the lung leads to several severe diseases such as fibrosis, chronic obstructive pulmonary disease and cancer. Noxious environmental aerosols are comprised of a gas and particulate phase representing highly complex chemical mixtures composed of myriads of compounds. Although some critical pollutants, foremost particulate matter (PM), could be linked to adverse health effects, a comprehensive understanding of relevant biological mechanisms and detrimental aerosol constituents is still lacking. Here, we employed a systems toxicology approach focusing on wood combustion, an important source for air pollution, and demonstrate a key role of the gas phase, specifically carbonyls, in driving adverse effects. Transcriptional profiling and biochemical analysis of human lung cells exposed at the air–liquid-interface determined DNA damage and stress response, as well as perturbation of cellular metabolism, as major key events. Connectivity mapping revealed a high similarity of gene expression signatures induced by wood smoke and agents prompting DNA-protein crosslinks (DPCs). Indeed, various gaseous aldehydes were detected in wood smoke, which promote DPCs, initiate similar genomic responses and are responsible for DNA damage provoked by wood smoke. Hence, systems toxicology enables the discovery of critical constituents of complex mixtures i.e. aerosols and highlights the role of carbonyls on top of particulate matter as an important health hazard.

1. Introduction

Air pollution, ambient (outdoor) and household (indoor), represents the major environmental risk factor to human health and is one of the prime causes for premature death (Allenet al. 2011; Cohenet al. 2017; Heft-Nealet al. 2018; Lelieveldet al. 2015). Since the Harvard Six Cities Study (Dockeryet al. 1993), a growing number of epidemiological studies have linked air pollution to adverse health effects such as

* Corresponding author at: Institute of Biological and Chemical Systems, Biological Information Processing, Karlsruhe Institute of Technology, Campus North, Eggenstein-Leopoldshafen, Germany
E-mail address: carsten.weiss@kit.edu (C. Weiss).
[1] www.hice-vi.eu.

https://doi.org/10.1016/j.envint.2023.108169
Received 28 November 2022; Received in revised form 19 July 2023; Accepted 22 August 2023
Available online 24 August 2023

respiratory and cardiovascular morbidity and mortality (Brunekreef and Holgate 2002; Cohenet al. 2017). However, the respective contribution of individual pollutants to the detrimental health effects as well as their chemical identity is poorly understood (Lelieveld and Pöschl 2017; Raaschou-Nielsenet al. 2016).

A main source of air pollution is the combustion of fossil fuels generating complex aerosols comprised of a particle and a gas phase. Important noxious gases in ambient air are ozone and nitrogen oxides, which are monitored along with respirable fine particulate matter smaller than 2.5 μm ($PM_{2.5}$) and different exposure limits are applied globally. Yet, combustion aerosols are comprised of myriads of compounds which are present in the gas phase and/or bound to particles. The chemical composition is highly variable and depends on many parameters such as the fuel source, combustion and environmental conditions and ageing. To complicate matters even further, the biological action of such dynamic and complex chemical mixtures is hard to address and hence not well known.

An important source of ambient air pollution in Europe and North America is residential heating with wood, particularly in the cold season (Linet al. 2018; WHO 2015). Due to climate policies, especially in the EU, biomass is touted as a renewable fuel and therefore wood combustion is favored in the coming decades. Even more pronounced is the impact of wood smoke on air pollution and human health in developing countries where wood is a dominant residential energy source for heating and cooking (Conibearet al. 2018; Naeheret al. 2007).Burning of solid fuels is often inefficient and incomplete which results in high emissions of harmful gaseous compounds and particulate matter. Besides inorganic material including toxic metals, these particles contain elemental carbon (soot) and organic compounds including hazardous polycyclic aromatic hydrocarbons (PAHs) (Dilgeret al. 2016). The gas phase of wood smoke mainly contains carbon monoxide, nitric and sulfur oxides as well as volatile organic compounds. There are a number of oxygenated organic compounds which are of toxicological concern such as aldehydes, alcohols and phenols (WHO 2015). Even in the emissions of modern masonry heaters and wood stoves, these substances can be detected albeit in reduced concentrations (Czechet al. 2018). Although some of the individual compounds are irritating, mutagenic and carcinogenic (WHO 2012; 2015; 2016a) it remains unclear to which extent, if any, they contribute to the overall detrimental health effects of wood smoke. Furthermore, the possible complex interaction of these various constituents (additive, synergistic or antagonistic) to drive adverse effects has not been investigated. Moreover, an ever-increasing sophisticated chemical analysis of aerosols reveals thousands of additional compounds with scarce knowledge on their biological activities (Czechet al. 2018; Weggleret al. 2016).

Systems biology approaches including phenotypic screens are increasingly used to uncover the mechanisms of action of mostly single compounds and are also embraced to support systems toxicology also known as toxicology of the 21st century (Bellet al. 2017; Kleinstreueret al. 2014). Differential regulation of transcripts, proteins and metabolites by chemical perturbants can be investigated at a global scale by OMICS technologies (Viantet al. 2019; Waters and Fostel 2004). Bioinformatic tools allow to discover individual as well as networks of pathways which are deregulated by toxicants (Fortinoet al. 2022; Wooet al. 2015). More and more databases are available which can be queried for hazard assessment of single chemicals and to extrapolate from in vitro experiments to the in vivo situation (Huanget al. 2016; Kohonenet al. 2017). Data is also compiled by text mining tools as in case of the Comparative Toxicogenomics Database (CTD) and potential relationships between certain chemicals or even chemical moieties, gene expression and human disease might be inferred (Duran-Frigolaet al. 2014; Davisetal. 2017). In the field of drug discovery, millions of gene expression profiles for thousands of mainly pharmaceuticals at different concentrations and time points were recorded which can be compared to the signatures of novel compounds to deduce their mode of action via the so-called connectivity map (CMAP) (Lambet al. 2006; Subramanianet al. 2017). Interestingly, in the field of hazard assessment the CMAP approach has rarely been employed. Connectivity mapping has been used as a tool to support read-across hypotheses (De Abrewet al. 2019). In the case of chemical carcinogenesis, in vitro transcriptomics data in human hepatocytes could indeed predict the hepatocarcinogenic potential for a suite of compounds in humans (Caimentet al. 2014). More recently, connectivity mapping was performed to establish predictive tools for ecotoxicology exploiting zebrafish and fathead minnow as model organisms (Wanget al. 2016).

So far, due to the lack of appropriate exposure technology a detailed understanding of the contribution of individual aerosol constituents to adverse effects in the lung is still scarce. Mostly the PM fraction was studied, which needs to be sampled and applied as suspension to biological test systems. However, such procedures often alter the physicochemical properties of particles and thus also their toxicological effects (Lacroixet al. 2018; Pauret al. 2011). In the present study, the impact of a complex aerosol i.e. wood smoke on the genomic response of human alveolar and bronchial lung epithelial cells was explored, as the alveolar and bronchial regions deep in the lung are the primary targets upon inhalation.. In contrast to simplistic, conventional submerged exposure, an improved air–liquid interface (ALI) exposure system was employed to assess adverse effects of the complete aerosol, including the gas phase (Mulhoptet al. 2016).Not only the effects of complete wood smoke but also of the gas phase after removal of PM were investigated by global mRNA-sequencing. The disturbance of affected cellular pathways predicted by bioinformatic analyses was verified by targeted analysis of selective markers with established biochemical and metabolomic assays. To determine the aerosol constituents dominating the molecular actions of wood smoke, the CMAP method was applied. Intriguingly, the gene expression signatures induced by the entire aerosol were very similar to those provoked by the gas phase. Whereas the selective genetic fingerprint triggered by PM could be mainly ascribed to PAHs, the gas phase more broadly initiated a DNA damage and stress response and altered cellular metabolism. The drugs which are prioritized by connectivity mapping, i.e. which share a similar gene expression profile with wood smoke, act via formation of DNA-protein crosslinks (DPC). As predicted by CMAP, wood smoke promotes DPCs and DNA damage in multiple airway epithelial cells. Chemical analysis of the gas phase reveals various aldehydes such as formaldehyde, which provoke similar genomic responses, promote DPCs and are indeed responsible for DNA damage provoked by wood smoke.

2. Methods

2.1. Materials

Materials and reagents were obtained from the following suppliers: Roswell Park Memorial Institute medium 1640 (RPMI), RPMI 1640 with 10 mM HEPES, cell culture medium supplements, Dulbecco's phosphate-buffered saline (DPBS): ThermoFisher Scientific (Dreieich, Germany); KGM medium, cell culture medium supplements: Lonza, Köln, Germany); Transwell® inserts with a 24 mm polyester membrane with 0.4 μm pores, Transwell® inserts with a 24 mm polycarbonate membrane, fetal bovine serum (FBS), LDH Cytotoxicity detection kit: Sigma-Aldrich (Taufkirchen, Germany); chemicals for sodium dodecylsulfate polyacrylamide gel electrophoresis (SDS-PAGE), chemicals for transmission electron microscopy (TEM): Carl Roth (Karlsruhe, Germany); peqGold Trifast total RNA preparation kit: VWR, Bruchsal, Germany); Immobilon-P PVDF membranes: Millipore (Eschborn, Germany); anti-MK2, anti-phospho p38 (Thr180/Tyr182), anti-phospho ERK1/2 (Thr202/Tyr204), anti-phospho JNK1/2 (Thr183/Tyr185), anti-phospho c-Jun (Ser63), and anti-phospho MK2 (Thr334): Cell Signalling (Frankfurt a.M., Germany), anti-PCNA (PC-10), anti-ERK1 (K-23), anti-p38 (c-20), anti-Lamin B (M20): Santa Cruz (Heidelberg, Germany), IRDye-700- and IRDye-800-labelled secondary antibodies: Biomol (Hamburg, Germany).

2.2. Aerosol generation and characterization

A 8 kW log wood stove (type "Toronto", Hase Kaminofenbau GmbH, Germany) was fired with beech logs and diluted with filtered ambient indoor air by a factor of 10 as previously described (Mulhoptet al. 2016). Beech logs with a humidity of less than 15 % were stored in the laboratory according to DIN EN ISO 17225-5. The oven fire was started about 1 h before cell exposure to achieve a stable operating temperature. During a 4 h cell exposure, between 5 and 7 kg firewood were burned in 5 to 6 batches with equal intervals. The aerosol in the conditioning reactor of the exposure system has been analysed using the Scanning Mobility Particle Sizer SMPS (Model 3934C-3 TSI Inc., Minnesota, USA) as described (Mulhoptet al. 2016). For analysis of metals and polycyclic aromatic hydrocarbons (PAHs), four parallel $PM_{2.5}$ filter samples were collected with a modified speciation sampler (Rupprecht & Patashnik 2300, Thermo Scientific, Waltham, USA) simultaneously and under the same dilution ratio as the aerosol for the cell exposure. PM samples were collected on quartz fiber filters (QFF, T293, Munktell, Sweden) and PTFE membrane filters (PFF, Zefluor 1 µm, Pall, USA). In case of SVOC analysis, only one quartz fiber filter was used. Carbonyl compounds from the gas phase were trapped by derivatisation with two 2,4-dinitrophenylhydrazine (DNPH) cartridges (Orbo 555, Sigma-Aldrich, Germany) placed in series before individual cell exposure positions.

2.3. Cells and exposure in the ALI system

Cell exposures were performed with the human alveolar epithelial cell line A549 and the human bronchial epithelial cell line BEAS-2B, both obtained from American Type Culture Collection (ATCC, Rockville, MD). A549 cells were maintained in RPMI 1640 supplemented with 10% (v/v) FBS, 100 U/mL penicillin, and 100 mg/mL streptomycin (Dilgeret al. 2016) and the BEAS-2B cells in complete KGM medium (Diabaté et al. 2011). Further details for exposure to aerosol are described (Mulhoptet al. 2016). Briefly, 24 h before exposure, 4×10^5 A549 cells or 5×10^5 BEAS-2B cells were seeded on 24 mm Transwell® inserts corresponding to a cell density of 8.6×10^4 or 1.1×10^5 cells/cm^2 growth area, respectively. Cells were exposed at the ALI in Vitrocell CF 6/3 modules for 4 h with a flow rate of 100 mL/min and a relative humidity of 85% using HEPES supplemented RPMI 1640 medium in the basolateral compartment. Several ALI systems use a flow rate of 5 or 10 mL/min to expose cells in a 24- or 12- well format. As such simple systems lack the possibility to control humidification to prevent dehydration of cells, the flow rate cannot be increased to e.g. 100 mL/min. However, with increased flow rates the deposition of particles is much more reproducible i.e. the standard deviation of the deposited mass decreases significantly (Adamsonet al. 2013). Therefore, in our ALI exposure system at KIT we have implemented a stable humidification to increase the flow rate up to 100 mL/min for proper aerosol characterization and reproducible deposition of particles. This is a compromise between the requirements of accurate aerosol measurements on the one hand and of a reasonably low flow rate to ensure viability of exposed cells on the other. That indeed cells are healthy and show no signs of adverse effects upon exposure to clean air at this flow rate has been demonstrated by us previously. To this end, different endpoints were monitored such as viability (AlamarBlue, WST-1 assay, cell counts), cytotoxicity (LDH release), genotoxicity (comet assay, alkaline unwinding) and markers of inflammation (IL-8) in cell lines such as A549, BEAS-2B or co-cultures of these with macrophages (Diabaté et al. 2020; Friesenet al. 2023; Mulhoptet al. 2016; Murugadosset al. 2021; Oeder et al. 2015) Although the flow rates in other ALI systems of 5 or 10 mL/min are much lower compared to 100 mL/min used in our system, the velocity of the air stream depends on the relative surface area of the exposed cells. Calculations for the different ALI set-ups show that the average velocity is between 2.9E and 03 to 7.4E-03 m/s for a 24- and 12-well insert exposed to 5 mL/min, whereas it is about 3.7E-03 m/s for a 6 well insert in our system (Supplementary Table S1). In essence, the velocities are in a similar range when comparing the different systems.

2.4. Chemical analysis

Particle bound organic species were analyzed with the in-situ derivatization thermal desorption method as described (Orascheet al. 2011). Dependent on particle load, filter punches of 4 to 20 mm^2 were spiked with isotope-labeled standards. After derivatization, samples were analyzed on a 60 m BPX-5 column (0.22 mm i.d., 0.25 µm film, SGE, Australia) with a Pegasus III TOFMS (LECO, USA). The thermal optical analysis of elemental carbon (EC) and organic carbon (OC) was performed with the IMPROVE-A protocol using transmission correction (Chowet al. 2011). Metal species were analyzed as described (Orascheet al. 2012) with the exception that only inductively coupled plasma – mass spectrometry (ICP-MS) was used. Carbonyl compounds were determined by eluting the 2,4-dinitrophenyhydrazin (DNPH) cartridges with acetonitrile followed by gas chromatography – mass spectrometry (GC–MS) analysis as described (Redaet al. 2015). By using two DNPH cartridges in series, sample break-through was excluded.

2.5. Transmission electron microscopy (TEM)

Wood smoke particles were deposited on TEM grids (Plano, SF162-6) which were placed on the Transwell membranes (Panaset al. 2014)and analysed by a transmission electron microscope (Zeiss 109 T, Oberkochen).

2.6. mRNA sequencing and differential expression analysis

After exposure, A549 cells were directly lysed in 500 µL Trizol reagent and total RNA was isolated according to the manufacturer's protocol. RNA from BEAS-2B cells was prepared from the interphase of samples processed for metabolite determination (see below). After removing remaining polar and organic phase from the interphase 500 µL Trifast was added and sample preparation continued as with A549 cells. All samples had RIN numbers $\gg$ 8 (Bioanalyser 2100, Agilent). 1 µg (A549) or 0.5 µg (BEAS-2B) RNA was used for preparation of individual libraries with TruSeq mRNA kit V2 (Illumina, San Diego, CA, USA). Size and concentration of sequencing libraries were determined on DNA-chip (Bioanalyser 2100, Agilent) and concentrations adjusted to 8 pM. Paired end reads (2×50 nucleotides) were obtained on a Hiseq1500 using SBS v3 kits (Illumina, San Diego, CA, USA). Cluster detection and base calling were performed using RTAv1.13 and quality of reads were assessed with CASAVA v1.8.1 (Illumina, San Diego, CA, USA). The mean Phred quality score was greater than 30 for all samples. The reads were mapped against the human genome (GRCh37) using topHat version 2.0.11(Kimet al. 2013)with the options "-r 180 –mate-std-dev 80 –b2-sensitive -–no-novel-juncs -a 5 -p 5 –library-type fr-unstranded" and using known exon junctions (Ensembl release 75). Gene expression was determined by counting for each gene the number of reads that overlapped known genes (Ensembl release 75) with HTSeq version 0.5.3p3 (Anderset al. 2013). Differential expression was computed using the R package DESeq2 (Anderset al. 2015). If not indicated otherwise, a transcript was considered to be differentially regulated if the adjusted p-value is < 0.001 and the absolute log2-fold change is ≥ 1. 3485 and 2099 DEGs were identified for A549 and BEAS-2B, respectively. As during the course of the project the genome annotation as well as the mapping software were updated, we re-analyzed our RNA sequencing data using the genome version GRCh38 and Ensembl release 108 together with STAR (Dobinet al. 2013) and confirmed the initially identified DEG and GO terms. Sample quality control metrics are provided in Supplementary Table S2 and Supplementary Fig S1.

2.7. Bioinformatic analyses

Correlations with NextBio Datasets: datasets related to combustion

areosols and genotoxins with diverse mode of actions were downloaded from the NextBio database during December 2016-February 2017. The data was used as retrieved, i.e. only significant DEG are included, but no further filtering criteria were applied. The data were compared to the top 2000 (by p-value) DEG after wood smoke exposure (aerosol vs control). The intersecting set of DEG (based on gene symbols present in both compared datasets) was used for correlation plots of the log2-fold changes.

Correlation with cigarette smoke exposure: eight-to-ten-week-old and twelve-month-old female C57BL/6 mice were whole-body-exposed to active 100% mainstream cigarette smoke for 50 min twice per day for 6 months as previously described (Conlonet al. 2020). Twenty-four hours after the last exposure to cigarette smoke, mice were killed. The right lung lobes were snap frozen in liquid nitrogen, homogenized and total RNA isolated and amplified using the Illumina TotalPrep RNA Amplification kit (Ambion), and finally hybridized to Mouse Ref-8 v2.0 Expression BeadChips (Illumina). Microarray data was retrieved from GEO (GSE125521) using the R package 'GEOquery'. The retrieved data was log-transformed and probes which did not achieve a hybridization intensity of 3 in at least 6 samples (out of 27 total) were removed from the expression set. Analysis of DEG was performed with all samples from the 6-month timepoint using limma (v 3.50.3) with R (v 4.1.3) using standard parameters. The intersecting set of DEG of wood smoke and cigarette smoke, with an adjusted p-value <=0.05 in each set, was used for plotting the correlation on the basis of identical gene symbols. In case multiple transcripts were represented by the same gene symbol, a single value was created by taking the mean. The top regulated 2000 DEGs in A549 cells in response to wood smoke were compared with the NextBio datasets of DEGs recorded for human prostate cancer cells (PC-3, number of genes for comparison 8823) exposed to camptothecin (11.4 μM, 6 h), for human spherocytic spleen cells (TK6, number of genes for comparison 4463) exposed to formaldehyde (200 μM, 4 h), of A549 cells (number of genes for comparison 5116) to acrolein (1 h) and of rats (number of genes for comparison 4914) exposed to formaldehyde via nasal instillation (200 μM, 6 h). In case of mice chronically exposed to cigarette smoke for 6 months, 1456 DEGs were compared to 7095 DEGs identified in A549 cells upon exposure to wood smoke.

GO-Term enrichment analysis: Ensembl Gene IDs of significant DEG were compared to a background list which consisted of all Ensembl Gene IDs which were counted at least once in each of the sequence samples using the web version of DAVID. Enriched GO-Terms are presented with adjusted p-values in the figures. Percentage of regulated transcripts refers to the fraction of DEG found within all Gene IDs in the background list which belong to the respective GO-Term.

Enrichment analysis using BioJupies: raw read count data of A549 cells exposed to complete and filtered wood smoke and clean air was uploaded to BioJupies (https://maayanlab.cloud/biojupies/) (Torreet al. 2018). Aerosol exposure and air controls were selected for DEG analysis and enrichment analysis (via Enrichr) was performed with the upregulated DEG using the automated workflow in BioJupies (accessible at https://amp.pharm.mssm.edu/Enrichr/enrich?dataset=99u4g).

2.8. LDH release

LDH release was analyzed as described in detail in (Mulhoptet al. 2016). Briefly, after exposure the LDH concentration in the cell culture medium beneath the insert membrane was determined and compared to lysed untreated cells, which served as a reference for 100% LDH release.

2.9. H2AX foci determination

Gamma-H2A foci formation was determined by immunostaining using the protocol described in (Kochet al. 2017) with some modifications for cells grown on insert membranes. After exposure, the cells were fixed by applying 4% formaldehyde/PBS directly in the Transwell inserts. Pieces of roughly 1 cm^2 were cut out and treated like cells grown on coverslips according to the immunostaining protocol. Microscopy slides were prepared by sandwiching membrane pieces with mounting medium (VectaMount, Vector Laboratories) between standard glass slides and cover slips. For each sample, 20 images were acquired using μManager 1.4.21 (Edelsteinet al. 2014) with a Leica DM IRE2 fluorescence microscope [63x objective and an ORCA-ER (Hamamatsu) camera]. Foci were counted automatically by the ScanR image analysis software (Olympus, Hamburg, Germany) by detecting focal gamma-H2AX signals within the nuclei. Selection criteria for foci (shape, signal intensity) were adjusted between experiments to result in comparable foci detection.

2.10. Quantification of DNA strand breaks by alkaline unwinding

Quantification of DNA strand breaks was performed as described in (Hartwiget al. 1996) with cells grown on Transwell inserts instead of petri dishes but using the same reagent volumes. Briefly, DNA was unwound at alkaline pH for 30 min, neutralized and sonicated. Resulting single stranded DNA (ssDNA) and double stranded DNA (dsDNA) were separated by column chromatography and quantified. Using the calibration from (Hartwiget al. 1996), the number of DNA strand breaks was calculated based on the fraction of double-stranded DNA of exposed cells relative to submerged control cells.

2.11. Immunoblotting

Immunoblotting was performed as described in (Dilgeret al. 2016). Cells were harvested using 100 μL lysis buffer per insert and lysates of 3 replicates were pooled. Bands were detected by analysis of fluorescently labelled secondary antibodies by using the Odyssey Scanner (LI-COR, Bad-Homburg, Germany).

2.12. Stable isotope assisted metabolomics

Cells were seeded in RPMI 1640 medium without glucose or without L-glutamine, with either 2.0 g/L U-$^{13}C_6$-Glucose (Euriso-Top, Saarbrücken) substituted for unlabeled glucose or 300 mg/L U-$^{13}C_5$-Glutamine (Campro, Berlin) substituted for unlabeled L-glutamine. Metabolite extraction was performed as described in detail by (Sapcariuet al. 2014). Quantification of metabolites was performed by GC–MS as described in (Wegneret al. 2013).

2.13. Determination of DNA-Protein-Crosslinks

DPCs (DNA-Protein-Crosslinks) were analyzed with an adapted protocol based on (Stingeleet al. 2016). All centrifugation steps were performed by 5 min of centrifugation at 4 °C and 2000 rcf, except where noted otherwise. After treatment, cells were washed with PBS (1.5 mL at the basolateral side, 1 mL at the apical side) followed by harvesting in 200 μL lysis buffer (2% SDS, 20 mM Tris pH 7.5) with a cell scraper and shock-freezing in liquid nitrogen. Directly after freezing or after overnight storage, samples were thawed in a shaker at 55 °C and 1000 rpm for 5 min. After sequential sonication with a probe-tip sonifier (5 pulses with 50% duty cycle and intensity 5), proteins were precipitated with 200 μL precipitation buffer (200 mM KCl, 20 mM Tris pH 7.5) and incubated on ice for 5 min. After 5 min centrifugation at 5 °C at maximum speed, 150 μL of the supernatant were kept for later determination of DNA concentration (=soluble DNA fraction) at 4 °C. The pellet was washed 3 times by the following procedure: solubilization in 200 μL precipitation buffer by shaking 5 min at 55 °C, incubation on ice for 5 min, centrifugation as before. After the last centrifugation step, the pellet was again solubilized in 200 μL precipitation buffer at 55 °C and proteins were digested by addition of 4 μL of 10 mg/mL Proteinase K (p6556, Sigma-Aldrich), final concentration 0.2 mg/mL) at 55 °C in the

shaker (1000 rpm). After 45 min, 10 μL of ultrapure BSA (50 mg/mL in H_2O, VWR 422381B) were added. Samples were incubated on ice for 5 min and centrifugated for 10 min instead of 5. 150 μL of supernatant were kept for determination of DNA concentration (=protein-bound DNA fraction).

Supernatants with the samples for soluble and protein-bound DNA were treated with 1.5 μL RNAse A R5503, Sigma-Aldrich) (final concentration 0.2 mg/mL) for 30 min at 37 °C. DNA content was analyzed with the picoGreen assay in the 96 well format by mixing 70 μL of sample with 70 μL 1:100 diluted picoGreen reagent in TE buffer and comparison with a calibration curve in the range of 0 to 2 μg/mL. Samples for soluble DNA were diluted 1:20 with PBS, while samples of protein-bound DNA were measured without additional dilution. Finally, for each sample, the fraction of protein-bound DNA to total DNA was calculated.

2.14. Statistics

The results are given as mean value ± standard deviation (SD) of independent experiments, unless explicitly differently described in the figure legends. Statistical analysis of differential gene expression (mRNA sequencing) was performed with DESeq2 as described above. The other statistical analyses were performed with R version 3.2.1 (R Foundation for Statistical Computing, Vienna, Austria) and significance values (p-values) for normal distributed data, unless explicitly stated otherwise in the legends, were determined using ANOVA and Dunnetts post hoc test (from the "multicomp" package) using the control treatments as a reference level. Non-normal distributed data were analysed by the Kruskal-Wallis test with Dunn's post hoc test (from the "FSA" package) using the Benjamini & Hochberg correction. The significance values were annotated in the figures as stated in the legends and results with $p < 0.05$ were considered significant.

3. Results

3.1. Aerosol characterization

Particle size and number distribution during a typical 4 h exposure experiment at the ALI (setup depicted in Fig. 1A and B) is shown in Fig. 1C. High fluctuations in both size and number are due to the batch-wise combustion of wood logs. The size distribution over the whole 4 h experiment is bimodal, with peaks around 40 and 110 nm (Fig. 1D). TEM analysis of deposited particles indicates partial agglomeration of primary particles of around 40 nm in accordance with the bimodal size distribution (Fig. 1E). The particle mass concentration was 1.16 ± 0.17 mg/m^3, determined gravimetrically by collecting particles on a filter from the same line that was used for cell exposure. The collected particles had a total carbon content of 41%, divided into 34% organic carbon (OC) and 7% elemental carbon (EC) (Fig. 1F). Further details on the chemical analysis of particle samples, including the content of metals and PAHs, can be found in Supplementary Tables S3 and S4. The deposited cellular particle dose, as determined via TEM image analysis and calibration to a fluorescent reference aerosol (Mulhoptet al. 2016) was estimated at 0.32 ± 0.02 μg/cm^2. In summary, the physico-chemical properties of PM generated by wood combustion in our experiments are similar to those described previously (Naeheret al. 2007; Orascheet al. 2012). The particle number concentration is about 10 to 100 - fold higher than detected in households in western countries using wood combustion for heating (Allenet al. 2011; Molnaret al. 2005; Wheeleret al. 2014) and are in the range found in indoor air in developing countries where wood smoke is also produced during cooking (Balakrishnanet al. 2002; McCrackenet al. 2007). Moreover, the deposited particle dose (~1000/cell) is equivalent to the calculated dose in the human lung after inhalation of heavily polluted air (Pauret al. 2011). Having established a physiological and toxicological relevant exposure system, we could start to analyze the biological impact of wood smoke with the additional aim to identify key pollutants.

3.2. Regulation of global gene expression is dominated by gaseous components in wood smoke

In order to characterize the effects of wood combustion aerosols on lung cells in an unbiased manner, we evaluated global changes in gene expression by next generation RNA sequencing. Exposures were performed at non-toxic concentrations to exclude indirect effects due to cell death (Supplementary Fig S2). The transcriptome of human alveolar (A549) and bronchial (BEAS-2B) epithelial cells was analyzed after ALI exposure to clean air, complete aerosol and particle-filtered aerosol (combustion gases). Differential expression analysis revealed over 2000 significantly regulated transcripts when A549 cells were treated with the complete aerosol in comparison to clean air (Fig. 2A). In striking contrast to expectations, the genomic response prompted by the gas phase was very similar to that of the complete aerosol (Fig. 2B, D), suggesting that gaseous combustion products of wood smoke are the

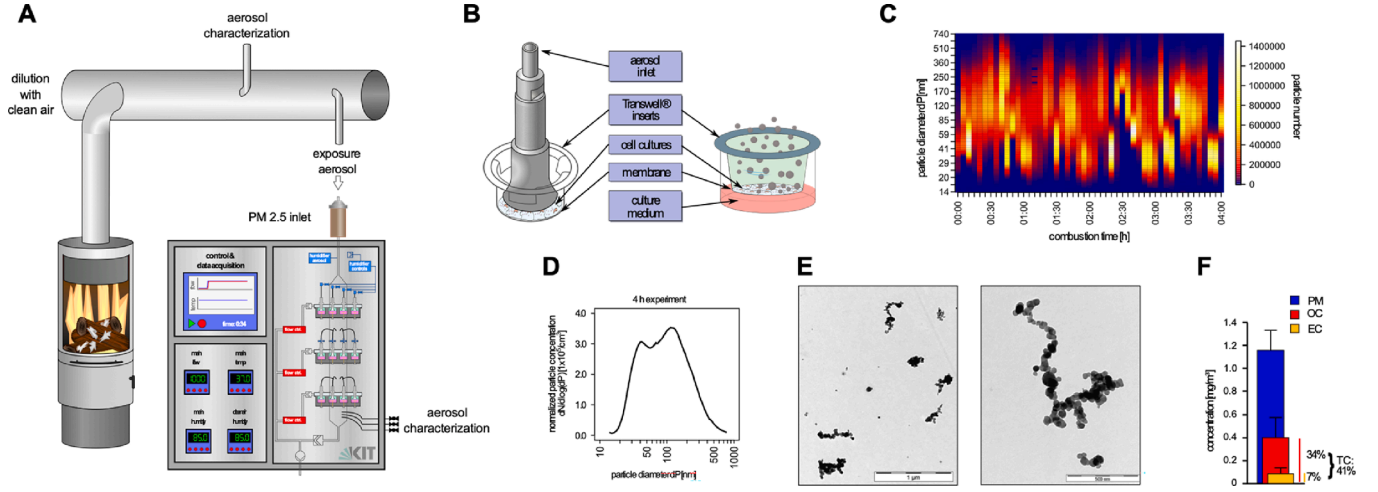

Fig. 1. The exhaust from a log wood stove was diluted 1:10 with filtered ambient air in a dilution tunnel and is passed into the exposure system (A), where cells are exposed homogeneously at the apical surface of a transwell membrane (B). The combustion produces a dynamic aerosol. Size and number distribution over time is depicted (C) with a bimodal size distribution, measured with SMPS (D). TEM images of representative samples to visualize particles at different magnification (E). Concentration of total particulates (PM), elemental (EC) and organic carbon (OC). Also, the total carbon (TC) content is calculated (F).

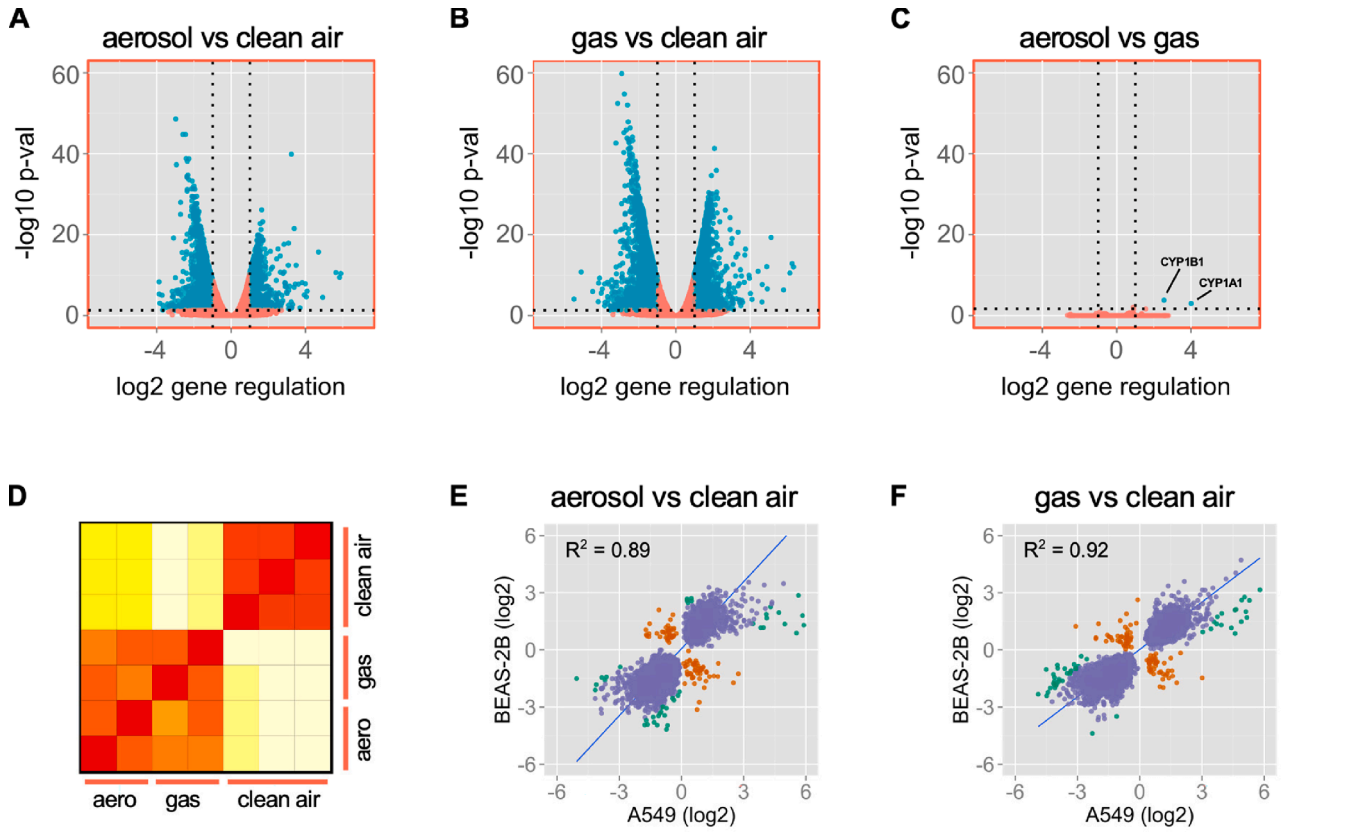

Fig. 2. A549 cells were exposed to clean air, filtered aerosol or complete aerosol for 4 h and differential gene expression was analysed using next generation sequencing. Volcano plots of the comparisons aerosol vs clean air (A), filtered aerosol (gas) vs clean air (B) and aerosol vs gas (C) are shown. Significantly deregulated genes are depicted as green dots. Distance matrix of analysed samples confirms the high similarity in response of cells exposed to the complete aerosol and filtered aerosol (D). The strength of correlation is indicated in the heat map by a colour code (light yellow-low correlation to dark red-high correlation). Comparison of alveolar (A549) and bronchial cells (BEAS-2B) shows a high similarity in DEG induced by the complete aerosol (E), as well as by the combustion gases only (F). R: Pearson correlation coefficient; purple dots: similar-regulated genes, green dots: genes regulated in the same direction yet with a different magnitude, red dots: oppositely regulated genes. (For interpretation of the references to colour in this figure legend, the reader is referred to the web version of this article.)

dominant drivers of differential gene expression. Indeed, only two genes, CYP1A1 and CYP1B1, are specifically induced by the complete aerosol but not in response to the gas phase alone (Fig. 2C). Hence, PM deposited at a high dose provoke only a limited yet distinct PAH response evidenced by upregulation of classical signature genes. These findings are in line with the chemical analysis of particles confirming the presence of planar PAHs (Supplementary Table S4) which are bona fide ligands of AhR and inducers of these xenobiotic responsible genes. Also, in BEAS-2B cells, the gas phase dominated the genomic response (Supplementary Fig S3). Even though both cell types originate from distinct areas of the lung, gene regulation induced by the complete aerosol or only the gas phase is nearly identical in alveolar A549 and bronchial BEAS-2B cells (Fig. 2E, F), with only very few genes regulated in opposite directions or with a strong difference in magnitude, some of which are depicted in (Supplementary Fig S4).

Next, we performed pathway enrichment analysis (PEA) to identify the biological processes affected by wood smoke exposure. The list of overrepresented gene ontology (GO) terms (Supplementary Table S5) covers many processes and pathways of toxicological relevance e.g. translation, transcription, DNA and RNA processing, cell cycle progression and metabolism. Specifically, exposure to wood smoke affected various DNA damage recognition and repair pathways (Fig. 3A, Supplementary Fig S5). In addition, mitogen-activated protein kinase (MAPK) signaling, a pathway which is triggered by environmental stress and DNA damage (Herrlichet al. 2008), seems to be affected (Fig. 3A and Supplementary Fig. S6). Finally, energy metabolism stands out as a central target of wood smoke intoxication (Fig. 3A and Supplementary Fig S7).

Air pollution is a main driver of human lung disease in particular inflammation, cancer, fibrosis and chronic obstructive pulmonary disease (COPD) (WHO 2016a). Therefore, deregulation of the DNA damage and repair pathway upon exposure of lung cells to wood smoke would be highly relevant, as this in vitro response is predictive for the action of genotoxic carcinogens in vivo (Caimentet al. 2014). Also, activation of MAPKs is of special interest as they regulate inflammation and the DNA damage response (Herrlichet al. 2008). Although PEA indicates perturbation of the aforementioned pathways most pertinent to inflammation and carcinogenesis, no GO terms related to fibrosis or COPD were identified. However, targeted manual analysis of the most highly deregulated genes (Supplementary Fig S8) indeed pinpoints numerous target genes which control epithelial-mesenchymal transition (EMT), a process of crucial importance for fibrosis and COPD, but also metastasis (Thiery and Sleeman 2006; Willis and Borok 2007).

More detailed bioinformatic gene set enrichment analysis via Enrichr (Kuleshovet al. 2016) identified transcription factors (TFs) of the AP-1, Egr, Snai and HES family by co-expression analysis (Supplementary Tab S6) and TF gene co-occurrence (Supplementary Tab S7 and Fig S9). The AP-1, Egr and Snai TFs are immediate early target genes responding to cellular stress which are regulated via the MAPK cascade and are involved in cancer progression, EMT and fibrosis (Pagel and Deindl 2012; Thiery and Sleeman 2006; Werniget al. 2017). Moreover, induction of multiple HES TFs indicates activation of the Notch pathway which is implicated in EMT (Espinoza and Miele 2013; Thiery and Sleeman 2006) and several lung diseases such as COPD, fibrosis and cancer (Zonget al. 2016).

In the following, we further corroborated and validated the impact of

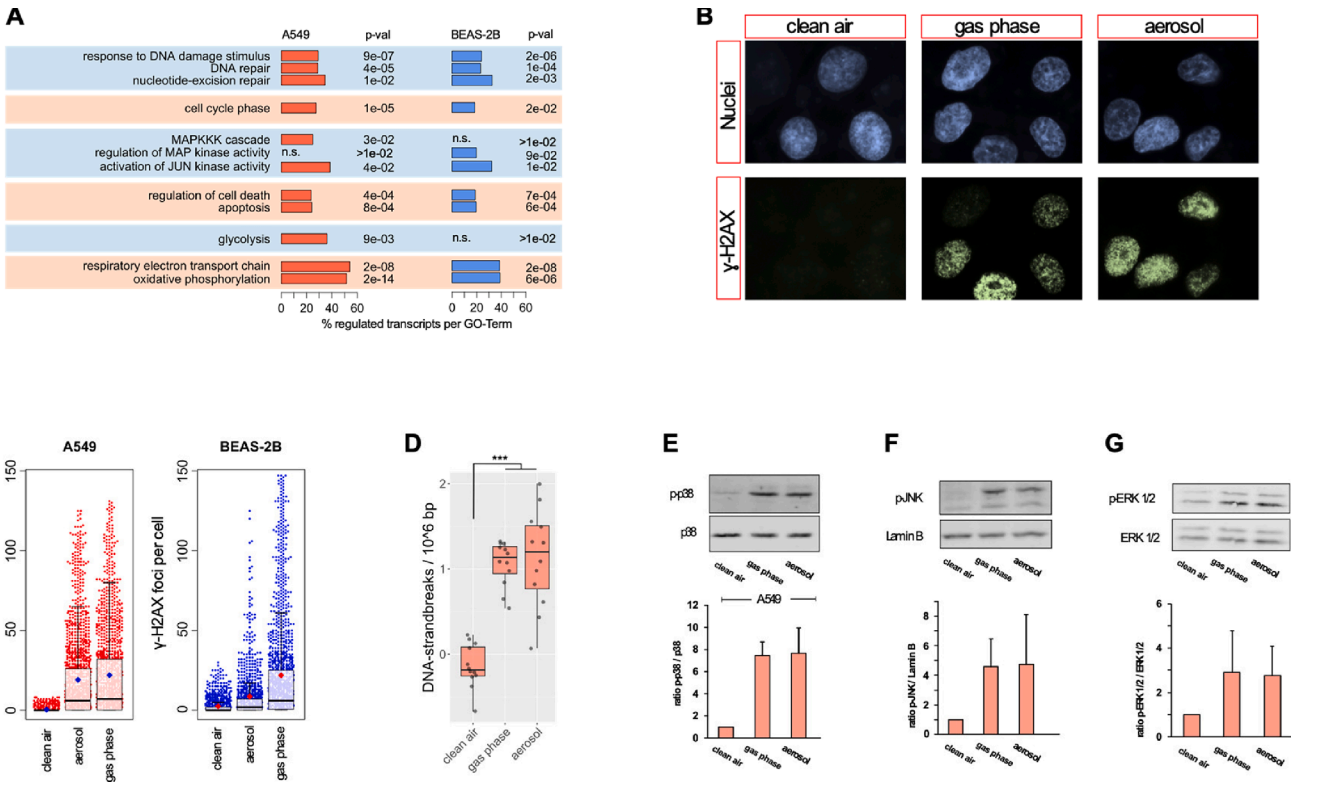

Fig. 3. GO-Term enrichment analysis of differentially regulated transcripts of cells exposed to the complete aerosol compared to clean air (A). γ-H2AX immunostaining and counterstaining with DAPI for identification of nuclei of A549 cells exposed to clean air, complete aerosol and particle-free gas phase (B) and quantification of γ-H2AX foci (C). Foci counts are the cumulative results from 3 experiments with 2 replicates each, with a total of at least 1300 analysed cells per condition. For better visualization, counts per cell beyond the 99th percentile were omitted. Boxplots show the mean (coloured square), median (bold line), first and third quartile (box) and 1.5-fold IQR (whiskers). DNA single strand breaks in A549 cells measured with alkaline unwinding (D), data from 3 experiments with 4 replicates each is shown as boxplots (C). *** = $p < 0.001$ according to Tukey's HSD post hoc test for ANOVA. Activation of p38 (E), JNK (F) and ERK (G) in A549 cells was monitored by western blotting. The phosphorylated (activated) kinase is detected by phospho-specific antibodies (p-p38, p-JNK, p-ERK1/2) and the quantified signal is normalized to the loading control (p38, Lamin B, ERK1/2). Quantification of the relative activation is shown below (3 experiments with 2 replicates each, mean and SD are depicted).

wood smoke on the selected pathways identified by PEA.

3.3. Biochemical validation of perturbed pathways indicated by transcriptomics

First, we assessed the potential of wood smoke to provoke DNA damage in human lung cells.

Induction of DNA double-strand breaks (DSBs) by the complete aerosol or simply the gas phase is evidenced by increased immunostaining for gamma-H2AX (Fig. 3B,C and Supplementary Fig S10-13), a well-established marker for the detection of DSBs (Rogakouet al. 1998) and which occured at a magnitude comparable to treatment with micromolar concentrations of the anticancer drug etoposide (Supplementary Fig S14). Furthermore, the gas phase prompted, similar to H_2O_2 (Supplementary Fig S15), a clear increase of DNA single-strand breaks (SSBs) as monitored by the alkaline unwinding assay (Fig. 3D).

Next, the induction of the MAPK pathway in response to wood smoke exposure was investigated. As predicted by PEA, all three members of the MAPK family (p38, JNK and ERK) and some of their substrates, specifically the AP-1 TF c-Jun, (Fig S16) were activated after treatment with either the complete aerosol or the gas phase (Fig. 3E).

Finally, wood smoke altered gene expression ascribed to the GO terms "glycolysis" and "oxidative phosphorylation". As differences in transcript levels encoding various enzymes do not necessarily predict metabolic activity (Heidenet al. 2009; ter Kuile and Westerhoff 2001) we investigated metabolic changes in more detail by stable isotope assisted metabolomics. As already observed for the transcriptomic and signaling responses above, A549 and BEAS-2B cells reacted very similar to the treatment with aerosol or particle-free gas phase concerning metabolic changes (Fig. 4A-C). However, the levels of citrate and lactate were changed divergently in the two cell lines. In summary, oxidative metabolism via the TCA cycle is suppressed by wood smoke exposure (Fig. 4A). Also, specifically in the lung cancer cell line A549, lactate is increased upon aerosol treatment indicative of enhanced glycolysis. A switch in cellular metabolism towards a dampened TCA cycle and enhanced glycolysis is reminiscent of the Warburg effect, which refers to the altered metabolism of cancer cells to adapt to limitations in oxygen supply and foster tumor growth. Interestingly, succinate accumulation, which has been linked to tumorigenesis (Kinget al. 2006),is also observed after aerosol intoxication (Fig. 4A-C).

3.4. Connectivity mapping suggests DNA-protein crosslinking agents as main drivers of differential gene expression

As the gas phase of the wood combustion aerosol is responsible for the observed changes in gene expression, we wanted to elucidate the chemical constituent(s) initiating the adverse response. Testing individual chemicals or even various mixtures thereof with respect to their effects on gene expression seemed to be tedious and not feasible, as the gas phase is a complex mixture of several hundreds of compounds (Naeheret al. 2007). Therefore, we preferred a chemical-genetic approach i.e. connectivity mapping to compare the gene expression profile (GEP) induced by wood smoke with over 7000 GEPs provoked by more than 1300 of selected pharmaceuticals with a known mode of

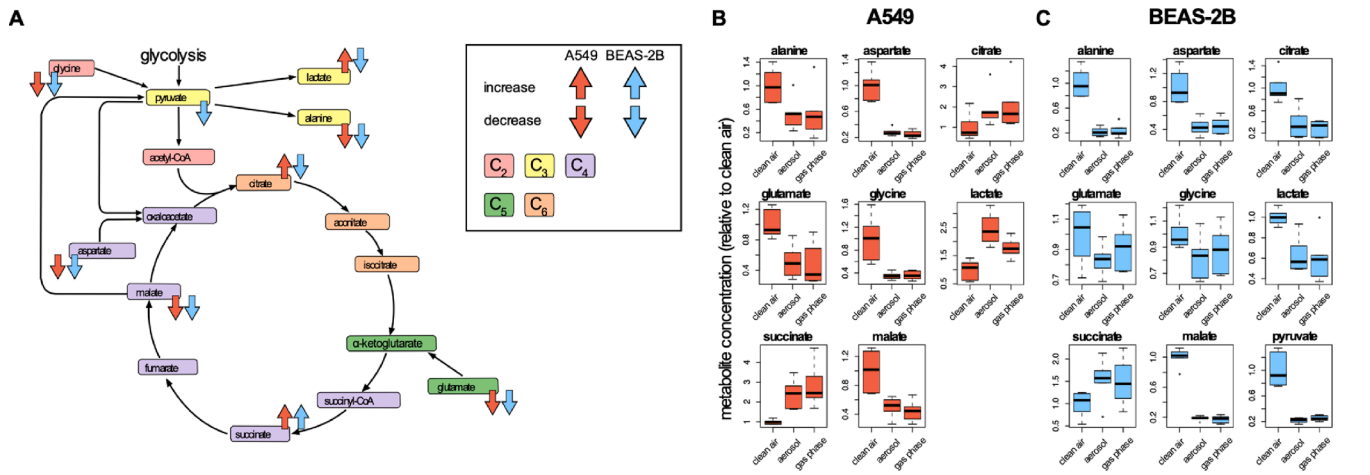

Fig. 4. Overview of qualitative changes in TCA metabolite concentrations after treatment with wood smoke aerosol (A). The number of C atoms (C_n) in the shown metabolites is indicated by the different colours. Metabolite concentrations, relative to controls, of A549 (B) and BEAS-2B (C) cells after exposure to filtered and complete aerosol. Shown are the median (bold line), range from first to third quartile (box) and 1.5-fold IQR (whiskers) of the means from 6 experiments with 3 replicate samples each.

action. CMAP analysis revealed a high similarity in the transcriptome response upon treatment with wood smoke (i.e. the gas phase) and DNA-protein crosslinking (DPC) agents. Specifically, several topoisomerase inhibitors (camptothecin, irinotecan, mitoxantrone) or azacitidine, which lead to covalent entrapment of their target enzymes i.e. topoisomerase and DNA methyltransferases, respectively, to DNA, ranked highest and shared the most similar gene expression signatures (Fig. 5A). Interestingly, other anticancer drugs acting also as genotoxins, yet by a different mechanism, elicit clearly distinguishable transcriptome responses compared to those induced by DPC agents. This suggests that DPC might be the decisive event prompting a highly selective pattern of gene expression (Supplementary Fig S17). Thus, we performed a targeted analysis of DPC chemicals in the gas phase of wood smoke focusing on carbonyls as potential lead candidates. Carbonyls react with free amino groups in proteins and DNA bases, which may result in protein–protein and DNA-protein crosslinks (DPCs) (Kawanishiet al. 2014).

3.5. *Aldehydes act as the main DPC and genotoxic agents in the gas phase of wood smoke*

Indeed, various carbonyls (e.g. formaldehyde (FA), acetaldehyde or acrolein) could be identified in the gas phase (Fig. 5B). To test our hypothesis that DPC originating from carbonyls in wood smoke are dominating the transcriptome response, we compared the top 2000 up- or downregulated genes with GEPs induced by known DPC agents. As already predicted by CMAP (Fig. 5A), camptothecin (Fig. 5C) also deregulated 1088 out of the 2000 genes targeted by wood smoke (overlap 54%) with a similarity in response, i.e. percentage of genes regulated in the same direction, of 91 %. Even more important, individual carbonyls assessed in different cell lines in vitro, such as FA (overlap 28%, similarity 93%) and acrolein (overlap 41%, similarity 92%), affected a large fraction of the most strongly regulated genes responding to wood smoke and the direction of the response (up or down) was highly similar (Fig. 5 D, E). Intranasal instillation of FA in rats still provoked a GEP including many of the target genes identified for wood smoke in human lung cells (overlap 24%, similarity 59%). Thus, a large proportion of the genes deregulated by wood smoke is as well affected by DPC agents in vitro and in vivo, suggesting that DPCs are key events to drive the toxicogenomic response after exposure to wood smoke. Another complex aerosol derived from biomass combustion comprised of multiple toxicants including aldehydes is cigarette smoke, which has been linked to several human diseases particularly affecting the lung. Therefore, we compared changes in GEPs provoked by acute exposure to wood smoke with those recently identified in mice chronically exposed to cigarette smoke (Conlonet al. 2020). Interestingly, 36 % of all the genes impacted by cigarette smoke in the murine lung after 6 months of exposure were also influenced by wood smoke in human cells after a few hours with a similarity in response of about 73% (Fig. 5G).

Finally, we wanted to verify the induction of DPC by wood smoke postulated by CMAP. Indeed, wood smoke (complete aerosol or the gas phase) promotes protein–protein as well as DNA-protein crosslinks similar to FA (Fig. 6 A,B and Fig S18, Fig S19) (Montaneret al. 2007). DPCs lead to replication stress and subsequently to increased DNA damage signaling evidenced by increased gamma-H2AX phosphorylation after treatment of cells with wood smoke or FA (Fig. 6C, Fig S20). Having established that wood smoke promotes DNA damage by provoking DPC, we set out to prove an essential role of aldehydes to trigger this molecular initiating event. Therefore, we quantitatively removed carbonyls from the exposure aerosol by DNPH-loaded trapping cartridges and demonstrated, that indeed the remaining gas phase no longer induced DPCs and gamma-H2AX foci (6B,C and Fig S21).

4. Discussion

Our transcriptome and biochemical analysis in two human lung cell lines exposed at the air–liquid interface could identify, for the first time, key pathways involved in lung diseases driven by air pollution. Mechanistically, exposure to wood smoke provokes stress signaling and a DNA damage response which are specifically related to genotoxicity, a known key event to promote carcinogenesis.

Hence, toxicogenomics combined with connectivity mapping enables the discovery of critical constituents of complex mixtures i.e. aerosols and highlights the role of carbonyls on top of particulate matter as important global health hazards. Thus, instead of exclusively relying on high-end techniques to monitor the ever-increasing chemical complexity of aerosols as a targeted approach to pinpoint known hazardous compounds without evidence of their biological impact, we advocate systems toxicology as a complementary strategy. The unbiased and simultaneous interrogation of all cellular pathways allows the effect-based identification of key toxicants amongst plenty of compounds by virtue of transcriptional profiling and similarity analysis, an approach which seems promising to clarify mechanisms of action for chemical mixtures in general and in the presented case those most pertinent to the field of air pollution. The development of an advanced

A

A549

substance	connectivity to WS
camptothecin	0.922
irinotecan	0.857
phenoxybenzamine	0.623
viomycin	-0.613
azacitidine	0.523

BEAS-2B

substance	connectivity to WS
camptothecin	0.925
azacitidine	0.776
mitoxantrone	0.705
dienestrole	0.687
irinotecan	0.687

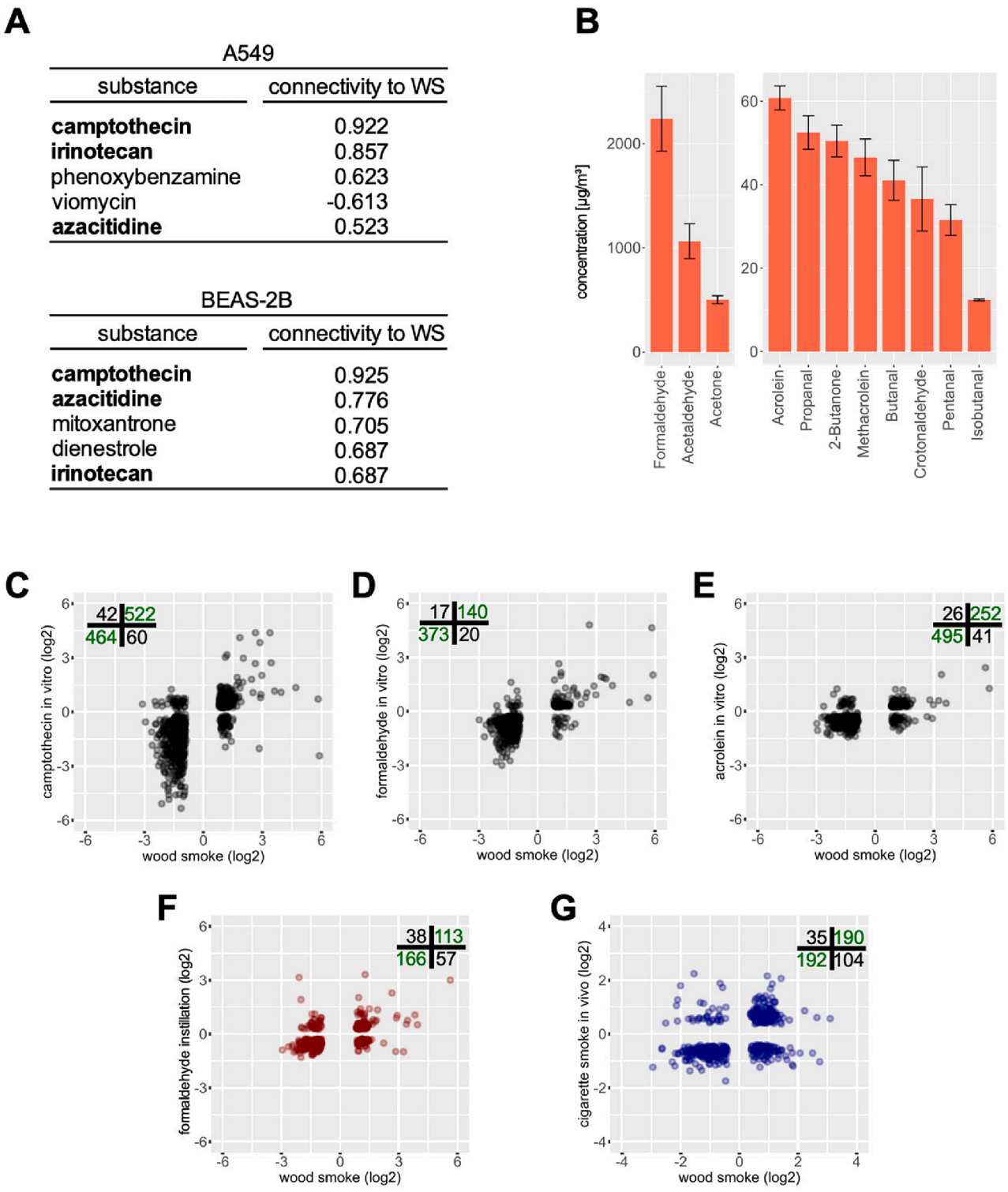

Fig. 5. Connectivity mapping reveals a high similarity of DEGs induced by wood smoke and DNA-protein crosslinking agents highlighted in bold (A). Carbonyl concentrations (means ± SEM of 8 samples from 2 independent 4 h combustion experiments) in the generated wood smoke determined by GC–MS (B). Note the different scale for the most prominent aldehydes shown in the left panel. Comparison of top regulated DEGs of A549 cells in response to wood smoke to DEGs recorded for in vitro exposure of human prostate cancer cells (PC-3) to camptothecin (C), of human spherocytic spleen cells (TK6) to formaldehyde (D) and of A549 cells to acrolein (E). Comparison to DEGs obtained from in vivo exposure of rats (nasal epithelium) to formaldehyde (F) and of mice (lung) exposed chronically to cigarette smoke (G). Numbers in quadrants indicate genes which are regulated in the same direction (depicted in green: lower left, downregulated; upper right, upregulated) or show opposite regulation (depicted in black). (For interpretation of the references to colour in this figure legend, the reader is referred to the web version of this article.)

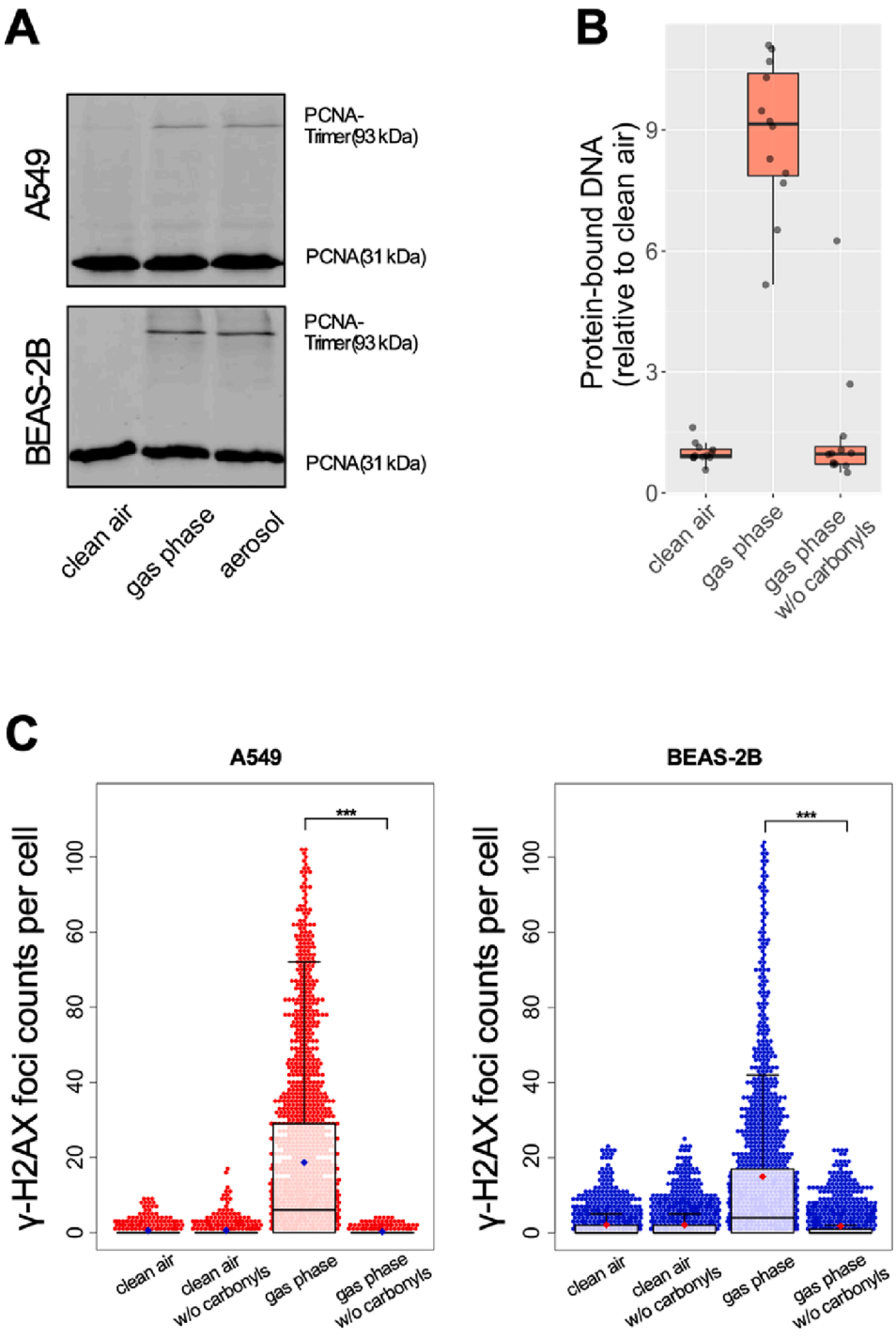

Fig. 6. Protein crosslinking (PCNA trimer formation) in A549 and BEAS-2B cells after exposure to complete wood smoke (aerosol) or only the gas phase for 4 h (A). A covalent protein–protein crosslink is evidenced by a shift of the molecular weight from 31 kDa of the PCNA monomer to 93 kDa of the PCNA trimer which is visualized by western blotting. DNA-protein-crosslinking in A549 cells exposed to the gas phase and the carbonyl-stripped gas phase (B), shown are the individual values, relative to the mean of controls, of at least 10 samples per condition from 4 independent experiments (dots) as well as their median (bold line), first and third quartiles (box) and 1.5-fold IQR (whiskers). Number of γ-H2AX foci per cell after immunostaining of A549 and BEAS-2B cells, exposed to clean air and particle-free gas phase, each with and without stripping of carbonyls (C). Counts are the cumulative results from 2 experiments with 1 or 2 replicates each, from a total of at least 1100 analysed cells per condition. Counts per cell beyond the 99th percentile were omitted for the sake of visualization. Boxplots show the mean (coloured square), median (bold line), first and third quartile (box) and 1.5-fold IQR (whiskers). ** = $p < 0.01$ according to Tukey's HSD post hoc test for ANOVA.

ALI system enabled us to interrogate the biological impact of a complex combustion derived aerosol on human lung cells employing OMICS analysis coupled with a suite of follow-up assays to validate the toxicity pathways predicted by computational tools. Worldwide millions of people are exposed daily to wood smoke, a main pollutant of ambient but also household air, and the health of many of them is potentially affected (Stoneret al. 2021). The premature death of millions of people per year has been linked to air pollution mainly due to respiratory and cardiovascular diseases. Specifically, in low and middle income countries, combustion of solid fuels such as wood for heating, cooking and lighting leads to high indoor air pollution impacting the health of particularly children and women(Stoneret al. 2021; WHO 2016b). Thus, it is surprising how little we know about key event relationships coupling certain key air pollutants or a mixture thereof present in wood smoke to molecular initiating events resulting in an adverse outcome. So far, the focus has been primarily on particulate matter (PM) which can be detected, quantified and sampled effectively. Chemical analysis of PM identified many toxicants including soot, PAHs, metals and others which most likely contribute to the enhanced morbidity and mortality associated with exposure to PM evidenced by epidemiological studies (WHO 2015; 2016a). Sampling of PM from polluted air allows direct administration of PM to biological test systems in vitro but also in vivo and therefore quite a few experimental studies have been performed to interrogate the underlying mechanism of action. Rather than directly causing toxicity, wood smoke particles serve as carriers of toxic compounds such as PAHs to cause cellular damage (Dilgeret al. 2016; WHO

2012). Based on this intensive amount of research on the health impact of PM, reduction of PM in ambient air has been recommended to minimize health risks. However, as the chemical composition of wood smoke not only includes PM but also the gas phase as well as semi-volatile compounds adsorbed to PM, there is an urgent need to not only unravel the complexity of systems perturbations provoked by wood smoke but also to identify additional key pollutants. Such knowledge should provide a basis to understand mechanisms of toxicity and allow the identification of critical constituents driving toxicity with the aim of mitigating the negative impact of one of the most abundant noxious aerosols (WHO 2015; 2016a).

In an interdisciplinary effort involving engineers, chemists, biologists and toxicologists we have developed an ALI exposure system to assess initially the biological effects of (nano)particles (Panaset al. 2014) to then also administer more complex combustion aerosols by directly linking our system to the aerosol source such as a wood stove or even a ship engine (Oeder et al. 2015). Here we went further and removed the particulate phase from the aerosol and thus were able to discriminate between particle and gas phase effects. Against our expectations, wood smoke particles triggered a very distinct response by upregulating only a few target genes of AhR which serves as a sensor of PAHs. The dominating response was due to volatile compounds, which is highly relevant for the risk assessment of combustion derived aerosols, as so far gas phase constituents are hardly considered as potential hazards and are often not accounted for in experimental designs. Obviously, part of the reason why the gas phase has been poorly investigated are technical reasons as in conventional submerged in vitro studies this could not be addressed. However, employing our advanced ALI technology combined with transcriptomics we were able to pinpoint the important role of the gas phase in the adverse response to wood smoke. Still, we were confronted with the problem that the gas phase is comprised of thousands of different compounds and thus represents a complicated mixture. The typical approach to identify toxic chemicals would be to perform in depth chemical analysis and based on available knowledge select candidates for individual toxicity testing. Indeed, safety assessment of chemicals in general relies on a case by case concept, meaning that every single compound is studied individually. This is one of the major road blocks in chemical safety, as this is not only time consuming and will take many years or decades, but also ignores the more realistic exposure to mixtures (Caporaleet al. 2022). In fact, mixture components might act additively via the same mode of action but also synergistically or additionally could antagonize each other. Hence, we did not pursue a chemistry driven analysis, but instead used a biology informed approach to reversely guide identification of possible candidates which could be connected to the observed biological perturbations. To this end we checked the utility of CMAP which again is designed to link individual chemicals, but not mixtures, and more specifically mostly drugs and small molecules but also genetic interference with specific GEPs and human disease. Similarity profiling of GEPs deregulated by wood smoke and its gas phase with those recorded for many drugs in different human cell lines suggested a high correlation with the activity of DPC inducing anticancer drugs. As carbonyls like FA and acetaldehyde are prominent in the gas phase and are known DPC agents (Grafstromet al. 1983) and classified as human carcinogens (Baanet al. 2009), we assumed that these could be the essential drivers for such a transcriptional profile. In support of this hypothesis, the GEPs after exposure to wood smoke were very similar to those obtained upon treatment with carbonyls in vitro and in vivo. More direct evidence that wood smoke can potently lead to DPCs and subsequently to DNA damage was provided by targeted biochemical assays. Bioinformatic analysis of the transcriptome data already posited genotoxicity as one of the main key events and was therefore in line with our direct validation of DPC activity of wood smoke. As DPC is a key event upstream of several processes involved in the DNA damage response and repair but also in case of unsuccessful repair gives rise to mutations which may lead to cancer, we removed carbonyls from the gas phase and were able to show their causative role in genotoxicity. Interestingly, also in another toxic aerosol derived from biomass combustion, i.e. tobacco smoke, aldehydes are found at high concentrations and have been shown to induce DNA lesions in mice and humans (Wenget al. 2018). The enhanced genotoxicity of and vulnerability to aldehydes due to genetic predisposition (Antonowiczet al. 2021; Tanet al. 2017) warrants a concept of personalized environmental medicine, including the assessment of individual exposure levels to chemicals, aka the personalized exposome (Jianget al. 2018). Clearly, hazard assessment of complex combustion aerosols as presented here needs to be accompanied by detailed risk assessment considering dosimetry and regioselective deposition of key pollutants, such as aldehydes, in the lung to eventually define critical thresholds of exposure (Hartwiget al. 2020; Rietjenset al. 2022).

Further development of the CMAP approach could entail integration of metabolomics and proteomics data to also consider such similarity in perturbation profiles of chemicals and mixtures in addition to GEPs. Moreover, systematic analysis of multi-omics profiles induced by chemicals, their mixtures as well as emerging pollutants in relevant biological models including ALI systems should be performed, to widen the data base of CMAP and broaden its impact also in the field of environmental medicine and chemical safety.

Finally, in order to reduce the global health burden linked to air pollution, emission rate targets not only need to focus on PM but should consider constituents of the gas phase such as aldehydes. Clearly, this is just the beginning to explore the complexity of entire combustion aerosols and highlights the relevance of the gas phase. However, the discrete effects of the other phases i.e. PM or the intermediate phase i.e. volatile compounds adsorbed to PM, deserve further attention as well. By building special ALI exposure devices PM could be deposited at enhanced levels, e.g. by electrostatic fields or the gas phase could be removed by denuders, and in this way a more detailed view of the contribution of different constituents of wood smoke or in general of ambient air pollution might be obtained. Also, other endpoints apart from genotoxicity have to be addressed such as respiratory infections and long-term consequences manifested in chronic pulmonary disease such as fibrosis or chronic obstructive pulmonary lung disease (Conlonet al. 2020). An even bigger challenge is to mimic extrapulmonary effects of air pollution in vitro. Although microphysiological systems exist to combine different organ-on-a-chip, the exposure of lung cells at the ALI with a simultaneous coupling to other organ-on-a-chip units has not yet been achieved (Yanget al. 2021). Clearly, advanced co-culture models have to be further established and exposed for weeks to months, and perturbation profiles need to be compared to in vivo studies designed to study these types of chronic disease, in order to infer critical chemical constituents but also toxicity pathways. Only such a mechanistic understanding of the health effects will allow regulation of critical emissions based on scientific evidence, and thus mitigate health risks and the global burden of disease associated with air pollution.

Declaration of Competing Interest

The authors declare that they have no known competing financial interests or personal relationships that could have appeared to influence the work reported in this paper.

Data availability

Data will be made available on request.

Acknowledgements

This work was partially funded by the Helmholtz Virtual Institute of Complex Molecular Systems in Environmental Health (HICE) via the Helmholtz Association of German Research Centers (HGF). S.C.S. was supported by a transnational access grant funded by the European Commission's 7th Framework Program research infrastructure project

QualityNano (Grant Agreement No: INFRA-2010-262163).

Data availability

All data generated or analysed during this study are included in this published article (and its Supplementary Information files/source data files). The RNAseq data generated in this study have been uploaded to Gene Expression Omnibus (GEO) with the following accession number: GSE228624.

Appendix A. Supplementary data

Supplementary data to this article can be found online at https://doi.org/10.1016/j.envint.2023.108169.

References

Adamson, J., Thorne, D., Dalrymple, A., Dillon, D., Meredith, C., 2013. Assessment of cigarette smoke particle deposition within the Vitrocell(R) exposure module using quartz crystal microbalances. Chem. Cent. J. 7, 50.

Allen, R.W., Carlsten, C., Karlen, B., Leckie, S., van Eeden, S., Vedal, S., Wong, I., Brauer, M., 2011. An Air Filter Intervention Study of Endothelial Function among Healthy Adults in a Woodsmoke-impacted Community. Am. J. Respir. Crit. Care Med. 183 (9), 1222–1230.

Anders, S., Pyl, P.T., Huber, W., 2015. HTSeq–a Python framework to work with high-throughput sequencing data. Bioinformatics 31:166-169.

Anders, S., McCarthy, D.J., Chen, Y., Okoniewski, M., Smyth, G.K., Huber, W., Robinson, M.D., 2013. Count-based differential expression analysis of RNA sequencing data using R and Bioconductor. Nat. Protoc. 8 (9), 1765–1786.

Antonowicz, S., Bodai, Z., Wiggins, T., Markar, S.R., Boshier, P.R., Goh, Y.M., Adam, M. E., Lu, H.N., Kudo, H., Rosini, F., Goldin, R., Moralli, D., Green, C.M., Peters, C.J., Habib, N., Gabra, H., Fitzgerald, R.C., Takats, Z., Hanna, G.B., 2021. Endogenous aldehyde accumulation generates genotoxicity and exhaled biomarkers in esophageal adenocarcinoma. Nat. Commun. 12(1):-.

Baan, R., Grosse, Y., Straif, K., Secretan, B., El Ghissassi, F., Bouvard, V., Benbrahim-Tallaa, L., Guha, N., Freeman, C., Galichet, L., Cogliano, V., 2009. A review of human carcinogens–Part F: chemical agents and related occupations. Lancet Oncol. 10 (12), 1143–1144.

Balakrishnan, K., Parikh, J., Sankar, S., Padmavathi, R., Srividya, K., Venugopal, V., Prasad, S., Pandey, V.L., 2002. Daily average exposures to respirable particulate matter from combustion of biomass fuels in rural households of southern India. Environ. Health Perspect. 110 (11), 1069–1075.

Bell, S.M., Phillips, J., Sedykh, A., Tandon, A., Sprankle, C., Morefield, S.Q., Shapiro, A., Allen, D., Shah, R., Maull, E.A., Casey, W.M., Kleinstreuer, N.C., 2017. An Integrated Chemical Environment to Support 21st-Century Toxicology. Environ. Health Perspect. 125, 054501.

Brunekreef, B., Holgate, S.T., 2002. Air pollution and health. Lancet 360 (9341), 1233–1242.

Caiment, F., Tsamou, M., Jennen, D., Kleinjans, J., 2014. Assessing compound carcinogenicity in vitro using connectivity mapping. Carcinogenesis 35 (1), 201–207.

Caporale, N., Leemans, M., Birgersson, L., Germain, P.-L., Cheroni, C., Borbély, G., Engdahl, E., Lindh, C., Bressan, R.B., Cavallo, F., Chorev, N.E., D'Agostino, G.A., Pollard, S.M., Rigoli, M.T., Tenderini, E., Tobon, A.L., Trattaro, S., Troglio, F., Zanella, M., Bergman, Å., Damdimopoulou, P., Jönsson, M., Kiess, W., Kitraki, E., Kiviranta, H., Nånberg, E., Öberg, M., Rantakokko, P., Rudén, C., Söder, O., Bornehag, C.-G., Demeneix, B., Fini, J.-B., Gennings, C., Rüegg, J., Sturve, J., Testa, G., 2022. From cohorts to molecules: Adverse impacts of endocrine disrupting mixtures. Science 375 (6582).

Chow, J.C., Watson, J.G., Robles, J., Wang, X., Chen, L.-W., Trimble, D.L., Kohl, S.D., Tropp, R.J., Fung, K.K., 2011. Quality assurance and quality control for thermal/optical analysis of aerosol samples for organic and elemental carbon. Anal. Bioanal. Chem. 401 (10), 3141–3152.

Cohen, A.J., Brauer, M., Burnett, R., Anderson, H.R., Frostad, J., Estep, K., Balakrishnan, K., Brunekreef, B., Dandona, L., Dandona, R., Feigin, V., Freedman, G., Hubbell, B., Jobling, A., Kan, H., Knibbs, L., Liu, Y., Martin, R., Morawska, L., Pope, C.A., Shin, H., Straif, K., Shaddick, G., Thomas, M., van Dingenen, R., van Donkelaar, A., Vos, T., Murray, C.J.L., Forouzanfar, M.H., 2017. Estimates and 25-year trends of the global burden of disease attributable to ambient air pollution: an analysis of data from the Global Burden of Diseases Study 2015. Lancet 389 (10082), 1907–1918.

Conibear, L., Butt, E.W., Knote, C., Arnold, S.R., Spracklen, D.V., 2018. Residential energy use emissions dominate health impacts from exposure to ambient particulate matter in India. Nat. Commun. 9, 617.

Conlon, T.M., John-Schuster, G., Heide, D., Pfister, D., Lehmann, M., Hu, Y., Ertuz, Z., Lopez, M.A., Ansari, M., Strunz, M., Mayr, C., Ciminieri, C., Costa, R., Kohlhepp, M. S., Guillot, A., Gunes, G., Jeridi, A., Funk, M.C., Beroshvili, G., Prokosch, S., Hetzer, J., Verleden, S.E., Alsafadi, H., Lindner, M., Burgstaller, G., Becker, L., Irmler, M., Dudek, M., Janzen, J., Goffin, E., Gosens, R., Knolle, P., Pirotte, B., Stoeger, T., Beckers, J., Wagner, D., Singh, I., Theis, F.J., de Angelis, M.H., O'Connor, T., Tacke, F., Boutros, M., Dejardin, E., Eickelberg, O., Schiller, H.B., Konigshoff, M., Heikenwalder, M., Yildirim, A.O., 2020. Inhibition of LT beta R signalling activates WNT-induced regeneration in lung. Nature 588(7836):151-+.

Czech, H., Miersch, T., Orasche, J., Abbaszade, G., Sippula, O., Tissari, J., Michalke, B., Schnelle-Kreis, J., Streibel, T., Jokiniemi, J., Zimmermann, R., 2018. Chemical composition and speciation of particulate organic matter from modern residential small-scale wood combustion appliances. Sci. Total Environ. 612, 636–648.

Davis, A.P., Grondin, C.J., Johnson, R.J., Sciaky, D., King, B.L., McMorran, R., Wiegers, J., Wiegers, T.C., Mattingly, C.J., 2017. The Comparative Toxicogenomics Database: update 2017. Nucleic Acids Res. 45 (D1), D972–D978.

De Abrew, K.N., Shan, Y.K., Wang, X., Krailler, J.M., Kainkaryam, R.M., Lester, C.C., Settivari, R.S., LeBaron, M.J., Naciff, J.M., Daston, G.P., 2019. Use of connectivity mapping to support read across: A deeper dive using data from 186 chemicals, 19 cell lines and 2 case studies. Toxicology 423, 84–94.

Diabate, S., Bergfeldt, B., Plaumann, D., Ubel, C., Weiss, C., 2011. Anti-oxidative and inflammatory responses induced by fly ash particles and carbon black in lung epithelial cells. Anal Bioanal Chem 401, 3197–3212.

Diabate, S., Armand, L., Murugadoss, S., Dilger, M., Fritsch-Decker, S., Schlager, C., Beal, D., Arnal, M.E., Biola-Clier, M., Ambrose, S., Mulhopt, S., Paur, H.R., Lynch, I., Valsami-Jones, E., Carriere, M., Weiss, C., 2020. Air-Liquid Interface Exposure of Lung Epithelial Cells to Low Doses of Nanoparticles to Assess Pulmonary Adverse Effects. Nanomaterials (Basel) 11.

Dilger, M., Orasche, J., Zimmermann, R., Paur, H.-R., Diabaté, S., Weiss, C., 2016. Toxicity of wood smoke particles in human A549 lung epithelial cells: the role of PAHs, soot and zinc. Arch. Toxicol. 90 (12), 3029–3044.

Dobin, A., Davis, C.A., Schlesinger, F., Drenkow, J., Zaleski, C., Jha, S., Batut, P., Chaisson, M., Gingeras, T.R., 2013. STAR: ultrafast universal RNA-seq aligner. Bioinformatics 29, 15–21.

Dockery, D.W., Pope, C.A., Xu, X., Spengler, J.D., Ware, J.H., Fay, M.E., Ferris, B.G., Speizer, F.E., 1993. An association between air pollution and mortality in six U.S. cities. N. Engl. J. Med. 329 (24), 1753–1759.

Duran-Frigola, M., Rossell, D., Aloy, P., 2014. A chemo-centric view of human health and disease. Nat. Commun. 5, 5676.

Edelstein, A.D., Tsuchida, M.A., Amodaj, N., Pinkard, H., Vale, R.D., Stuurman, N., 2014. Advanced methods of microscope control using muManager software. J. Biol. Methods 1.

Espinoza, I., Miele, L., 2013. Deadly crosstalk: Notch signaling at the intersection of EMT and cancer stem cells. Cancer Lett. 341 (1), 41–45.

Fortino, V., Kinaret, P.A.S., Fratello, M., Serra, A., Saarimaki, L.A., Gallud, A., Gupta, G., Vales, G., Correia, M., Rasool, O., Ytterberg, J., Monopoli, M., Skoog, T., Ritchie, P., Moya, S., Vazquez-Campos, S., Handy, R., Grafstrom, R., Tran, L., Zubarev, R., Lahesmaa, R., Dawson, K., Loeschner, K., Larsen, E.H., Krombach, F., Norppa, H., Kere, J., Savolainen, K., Alenius, H., Fadeel, B., Greco, D., 2022. Biomarkers of nanomaterials hazard from multi-layer data. Nat. Commun. 13, 3798.

Friesen, A., Fritsch-Decker, S., Mülhopt, S., Quarz, C., Mahl, J., Baumann, W., Hauser, M., Wexler, M., Schlager, C., Gutmann, B., Krebs, T., Goßmann, A.-K., Weis, F., Hufnagel, M., Stapf, D., Hartwig, A., Weiss, C., 2023. Comparing the Toxicological Responses of Pulmonary Air-Liquid Interface Models upon Exposure to Differentially Treated Carbon Fibers. Int. J. Mol. Sci. 24 (3), 1927.

Grafstrom, R.C., Fornace, A.J., Autrup, H., Lechner, J.F., Harris, C.C., 1983. Formaldehyde damage to DNA and inhibition of DNA repair in human bronchial cells. Science 220 (4593), 216–218.

Hartwig, A., Dally, H., Schlepegrell, R., 1996. Sensitive analysis of oxidative DNA damage in mammalian cells: use of the bacterial Fpg protein in combination with alkaline unwinding. Toxicol. Lett. 88, 85–90.

Hartwig, A., Arand, M., Epe, B., Guth, S., Jahnke, G., Lampen, A., Martus, H.-J., Monien, B., Rietjens, I.M.C.M., Schmitz-Spanke, S., Schriever-Schwemmer, G., Steinberg, P., Eisenbrand, G., 2020. Mode of action-based risk assessment of genotoxic carcinogens. Arch. Toxicol. 94 (6), 1787–1877.

Heft-Neal, S., Burney, J., Bendavid, E., Burke, M., 2018. Robust relationship between air quality and infant mortality in Africa. Nature 559 (7713), 254–258.

Heiden, M.G.V., Cantley, L.C., Thompson, C.B., 2009. Understanding the Warburg Effect: The Metabolic Requirements of Cell Proliferation. Science 324 (5930), 1029–1033.

Herrlich, P., Karin, M., Weiss, C., 2008. Supreme EnLIGHTenment: damage recognition and signaling in the mammalian UV response. Mol. Cell 29 (3), 279–290.

Huang, R., Xia, M., Sakamuru, S., Zhao, J., Shahane, S.A., Attene-Ramos, M., Zhao, T., Austin, C.P., Simeonov, A., 2016. Modelling the Tox21 10 K chemical profiles for in vivo toxicity prediction and mechanism characterization. Nat. Commun. 7, 10425.

Jiang, C., Wang, X., Li, X., Inlora, J., Wang, T., Liu, Q., Snyder, M., 2018. Dynamic Human Environmental Exposome Revealed by Longitudinal Personal Monitoring. Cell 175 (1), 277–291.e31.

Kawanishi, M., Matsuda, T., Yagi, T., 2014. Genotoxicity of formaldehyde: molecular basis of DNA damage and mutation. Front. Environ. Sci. 2.

Kim, D., Pertea, G., Trapnell, C., Pimentel, H., Kelley, R., Salzberg, S.L., 2013. TopHat2: accurate alignment of transcriptomes in the presence of insertions, deletions and gene fusions. Genome Biol 14, R36.

King, A., Selak, M.A., Gottlieb, E., 2006. Succinate dehydrogenase and fumarate hydratase: linking mitochondrial dysfunction and cancer. Oncogene 25 (34), 4675–4682.

Kleinstreuer, N.C., Yang, J., Berg, E.L., Knudsen, T.B., Richard, A.M., Martin, M.T., Reif, D.M., Judson, R.S., Polokoff, M., Dix, D.J., Kavlock, R.J., Houck, K.A., 2014. Phenotypic screening of the ToxCast chemical library to classify toxic and therapeutic mechanisms. Nat. Biotechnol. 32 (6), 583–591.

Koch, B., Maser, E., Hartwig, A., 2017. Low concentrations of antimony impair DNA damage signaling and the repair of radiation-induced DSB in HeLa S3 cells. Arch. Toxicol. 91 (12), 3823–3833.

Kohonen, P., Parkkinen, J.A., Willighagen, E.L., Ceder, R., Wennerberg, K., Kaski, S., Grafstrom, R.C., 2017. A transcriptomics data-driven gene space accurately predicts liver cytopathology and drug-induced liver injury. Nat. Commun. 8, 15932.
Kuleshov, M.V., Jones, M.R., Rouillard, A.D., Fernandez, N.F., Duan, Q., Wang, Z., Koplev, S., Jenkins, S.L., Jagodnik, K.M., Lachmann, A., McDermott, M.G., Monteiro, C.D., Gundersen, G.W., Ma'ayan, A., 2016. Enrichr: a comprehensive gene set enrichment analysis web server 2016 update. Nucleic Acids Res. 44 (W1), W90–W97.
Lacroix, G., Koch, W., Ritter, D., Gutleb, A.C., Larsen, S.T., Loret, T., Zanetti, F., Constant, S., Chortarea, S., Rothen-Rutishauser, B., Hiemstra, P.S., Frejafon, E., Hubert, P., Gribaldo, L., Kearns, P., Aublant, J.-M., Diabaté, S., Weiss, C., de Groot, A., Kooter, I., 2018. Air-Liquid Interface In Vitro Models for Respiratory Toxicology Research: Consensus Workshop and Recommendations. Appl In Vitro Toxicol 4 (2), 91–106.
Lamb, J., Crawford, E.D., Peck, D., Modell, J.W., Blat, I.C., Wrobel, M.J., Lerner, J., Brunet, J.-P., Subramanian, A., Ross, K.N., Reich, M., Hieronymus, H., Wei, G., Armstrong, S.A., Haggarty, S.J., Clemons, P.A., Wei, R.u., Carr, S.A., Lander, E.S., Golub, T.R., 2006. The Connectivity Map: using gene-expression signatures to connect small molecules, genes, and disease. Science 313 (5795), 1929–1935.
Lelieveld, J., Evans, J.S., Fnais, M., Giannadaki, D., Pozzer, A., 2015. The contribution of outdoor air pollution sources to premature mortality on a global scale. Nature 525 (7569), 367–371.
Lelieveld, J., Pöschl, U., 2017. Chemists can help to solve the air-pollution health crisis. Nature 551 (7680), 291–293.
Lin, C.S., Huang, R.J., Ceburnis, D., Buckley, P., Preissler, J., Wenger, J., Rinaldi, M., Facchini, M.C., O'Dowd, C., Ovadnevaite, J., 2018. Extreme air pollution from residential solid fuel burning. Nat. Sustainability 1 (9), 512–517.
McCracken, J.P., Smith, K.R., Diaz, A., Mittleman, M.A., Schwartz, J., 2007. Chimney stove intervention to reduce long-term wood smoke exposure lowers blood pressure among Guatemalan women. Environ. Health Perspect. 115 (7), 996–1001.
Molnar, P., Gustafson, P., Johannesson, S., Boman, J., Barregard, L., Sallsten, G., 2005. Domestic wood burning and PM2.5 trace elements: Personal exposures, indoor and outdoor levels. Atmos. Environ. 39 (14), 2643–2653.
Montaner, B., O'Donovan, P., Reelfs, O., Perrett, C.M., Zhang, X., Xu, Y.-Z., Ren, X., Macpherson, P., Frith, D., Karran, P., 2007. Reactive oxygen-mediated damage to a human DNA replication and repair protein. EMBO Rep. 8 (11), 1074–1079.
Mulhopt, S., Dilger, M., Diabate, S., Schlager, C., Krebs, T., Zimmermann, R., Buters, J., Oeder, S., Wascher, T., Weiss, C., Paur, H.R., 2016. Toxicity testing of combustion aerosols at the air-liquid interface with a self-contained and easy-to-use exposure system. J. Aerosol Sci 96, 38–55.
Murugadoss, S., Mulhopt, S., Diabate, S., Ghosh, M., Paur, H.R., Stapf, D., Weiss, C., Hoet, P.H., 2021. Agglomeration State of Titanium-Dioxide (TiO(2)) Nanomaterials Influences the Dose Deposition and Cytotoxic Responses in Human Bronchial Epithelial Cells at the Air-Liquid Interface. Nanomaterials (Basel) 11.
Naeher, L.P., Brauer, M., Lipsett, M., Zelikoff, J.T., Simpson, C.D., Koenig, J.Q., Smith, K. R., 2007. Woodsmoke health effects: a review. Inhal Toxicol 19, 67–106.
Oeder, S., Kanashova, T., Sippula, O., Sapcariu, S.C., Streibel, T., Arteaga-Salas, J.M., Passig, J., Dilger, M., Paur, H.-R., Schlager, C., Mülhopt, S., Diabaté, S., Weiss, C., Stengel, B., Rabe, R., Harndorf, H., Torvela, T., Jokiniemi, J.K., Hirvonen, M.-R., Schmidt-Weber, C., Traidl-Hoffmann, C., BéruBé, K.A., Wlodarczyk, A.J., Prytherch, Z., Michalke, B., Krebs, T., Prévôt, A.S.H., Kelbg, M., Tiggesbäumker, J., Karg, E., Jakobi, G., Scholtes, S., Schnelle-Kreis, J., Lintelmann, J., Matuschek, G., Sklorz, M., Klingbeil, S., Orasche, J., Richthammer, P., Müller, L., Elsasser, M., Reda, A., Gröger, T., Weggler, B., Schwemer, T., Czech, H., Rüger, C.P., Abbaszade, G., Radischat, C., Hiller, K., Buters, J.T.M., Dittmar, G., Zimmermann, R., Ahmad, S., 2015;10(6):-.. Particulate Matter from Both Heavy Fuel Oil and Diesel Fuel Shipping Emissions Show Strong Biological Effects on Human Lung Cells at Realistic and Comparable In Vitro Exposure Conditions. PLoS One 10 (6), e0126536.
Orasche, J., Schnelle-Kreis, J., Abbaszade, G., Zimmermann, R., 2011. Technical Note: In-situ derivatization thermal desorption GC-TOFMS for direct analysis of particle-bound non-polar and polar organic species. Atmos. Chem. Phys. 11 (17), 8977–8993.
Orasche, J., Seidel, T., Hartmann, H., Schnelle-Kreis, J., Chow, J.C., Ruppert, H., Zimmermann, R., 2012. Comparison of Emissions from Wood Combustion. Part 1: Emission Factors and Characteristics from Different Small-Scale Residential Heating Appliances Considering Particulate Matter and Polycyclic Aromatic Hydrocarbon (PAH)-Related Toxicological Potential of Particle-Bound Organic Species. Energy Fuel 26 (11), 6695–6704.
Pagel, J.I., Deindl, E., 2012. Disease Progression Mediated by Egr-1 Associated Signaling in Response to Oxidative Stress. Int. J. Mol. Sci. 13 (10), 13104–13117.
Panas, A., Comouth, A., Saathoff, H., Leisner, T., Al-Rawi, M., Simon, M., Seemann, G., Dossel, O., Mulhopt, S., Paur, H.R., Fritsch-Decker, S., Weiss, C., Diabate, S., 2014. Silica nanoparticles are less toxic to human lung cells when deposited at the air-liquid interface compared to conventional submerged exposure. Beilstein J. Nanotechnol. 5, 1590–1602.
Paur, H.R., Cassee, F.R., Teeguarden, J., Fissan, H., Diabate, S., Aufderheide, M., Kreyling, W.G., Hanninen, O., Kasper, G., Riediker, M., Rothen-Rutishauser, B., Schmid, O., 2011. In-vitro cell exposure studies for the assessment of nanoparticle toxicity in the lung-A dialog between aerosol science and biology. J. Aerosol Sci 42 (10), 668–692.
Raaschou-Nielsen, O., Beelen, R., Wang, M., Hoek, G., Andersen, Z.J., Hoffmann, B., Stafoggia, M., Samoli, E., Weinmayr, G., Dimakopoulou, K., Nieuwenhuijsen, M., Xun, W.W., Fischer, P., Eriksen, K.T., Sorensen, M., Tjonneland, A., Ricceri, F., de Hoogh, K., Key, T., Eeftens, M., Peeters, P.H., Bueno-de-Mesquita, H.B., Meliefste, K., Oftedal, B., Schwarze, P.E., Nafstad, P., Galassi, C., Migliore, E., Ranzi, A., Cesaroni, G., Badaloni, C., Forastiere, F., Penell, J., De Faire, U., Korek, M., Pedersen, N., Ostenson, C.G., Pershagen, G., Fratiglioni, L., Concin, H., Nagel, G., Jaensch, A., Ineichen, A., Naccarati, A., Katsoulis, M., Trichpoulou, A., Keuken, M., Jedynska, A., Kooter, I.M., Kukkonen, J., Brunekreef, B., Sokhi, R.S., Katsouyanni, K., Vineis, P., 2016. Particulate matter air pollution components and risk for lung cancer. Environ. Int. 87, 66–73.
Reda, A.A., Czech, H., Schnelle-Kreis, J., Sippula, O., Orasche, J., Weggler, B., Abbaszade, G., Arteaga-Salas, J.M., Kortelainen, M., Tissari, J., Jokiniemi, J., Streibel, T., Zimmermann, R., 2015. Analysis of Gas-Phase Carbonyl Compounds in Emissions from Modern Wood Combustion Appliances: Influence of Wood Type and Combustion Appliance. Energy Fuel 29 (6), 3897–3907.
Rietjens, I.M.C.M., Michael, A., Bolt, H.M., Siméon, B., Andrea, H., Nils, H., Christine, K., Angela, M., Gloria, P., Daniel, R., Natalie, T., Gerhard, E., 2022. The role of endogenous versus exogenous sources in the exposome of putative genotoxins and consequences for risk assessment. Arch. Toxicol. 96 (5), 1297–1352.
Rogakou, E.P., Pilch, D.R., Orr, A.H., Ivanova, V.S., Bonner, W.M., 1998. DNA double-stranded breaks induce histone H2AX phosphorylation on serine 139. J. Biol. Chem. 273 (10), 5858–5868.
Sapcariu, S.C., Kanashova, T., Weindl, D., Ghelfi, J., Dittmar, G., Hiller, K., 2014. Simultaneous extraction of proteins and metabolites from cells in culture. MethodsX 1, 74–80.
Stingele, J., Bellelli, R., Alte, F., Hewitt, G., Sarek, G., Maslen, S.L., Tsutakawa, S.E., Borg, A., Kjaer, S., Tainer, J.A., Skehel, J.M., Groll, M., Boulton, S.J., 2016. Mechanism and Regulation of DNA-Protein Crosslink Repair by the DNA-Dependent Metalloprotease SPRTN. Mol. Cell 64 (4), 688–703.
Stoner, O., Lewis, J., Martinez, I.L., Gumy, S., Economou, T., Adair-Rohani, H., 2021. Household cooking fuel estimates at global and country level for 1990 to 2030. Nature Communications 12 (1).
Subramanian, A., Narayan, R., Corsello, S.M., Peck, D.D., Natoli, T.E., Lu, X., Gould, J., Davis, J.F., Tubelli, A.A., Asiedu, J.K., Lahr, D.L., Hirschman, J.E., Liu, Z., Donahue, M., Julian, B., Khan, M., Wadden, D., Smith, I.C., Lam, D., Liberzon, A., Toder, C., Bagul, M., Orzechowski, M., Enache, O.M., Piccioni, F., Johnson, S.A., Lyons, N.J., Berger, A.H., Shamji, A.F., Brooks, A.N., Vrcic, A., Flynn, C., Rosains, J., Takeda, D.Y., Hu, R., Davison, D., Lamb, J., Ardlie, K., Hogstrom, L., Greenside, P., Gray, N.S., Clemons, P.A., Silver, S., Wu, X., Zhao, W.N., Read-Button, W., Wu, X., Haggarty, S.J., Ronco, L.V., Boehm, J.S., Schreiber, S.L., Doench, J.G., Bittker, J.A., Root, D.E., Wong, B., Golub, T.R., 2017. A Next Generation Connectivity Map: L1000 Platform and the First 1,000,000 Profiles. Cell 171, 1437–1452e1417.
Tan, S.L.W., Chadha, S., Liu, Y.S., Gabasova, E., Perera, D., Ahmed, K., Constantinou, S., Renaudin, X., Lee, M., Aebersold, R., Venkitaraman, A.R., 2017. Class of Environmental and Endogenous Toxins Induces BRCA2 Haploinsufficiency and Genome Instability. Cell 169 (6), 1105.
ter Kuile, B.H., Westerhoff, H.V., 2001. Transcriptome meets metabolome: hierarchical and metabolic regulation of the glycolytic pathway. FEBS Lett. 500 (3), 169–171.
Thiery, J.P., Sleeman, J.P., 2006. Complex networks orchestrate epithelial-mesenchymal transitions. Nat. Rev. Mol. Cell Biol. 7 (2), 131–142.
Torre, D., Lachmann, A., Ma'ayan, A., 2018. BioJupies: Automated Generation of Interactive Notebooks for RNA-Seq Data Analysis in the Cloud. Cell Syst. 7 (5), 556–561.e3.
Viant, M.R., Ebbels, T.M.D., Beger, R.D., Ekman, D.R., Epps, D.J.T., Kamp, H., Leonards, P.E.G., Loizou, G.D., MacRae, J.I., van Ravenzwaay, B., Rocca-Serra, P., Salek, R.M., Walk, T., Weber, R.J.M., 2019. Use cases, best practice and reporting standards for metabolomics in regulatory toxicology. Nat. Commun. 10.
Wang, R.L., Biales, A.D., Garcia-Reyero, N., Perkins, E.J., Villeneuve, D.L., Ankley, G.T., Bencic, D.C., 2016. Fish connectivity mapping: linking chemical stressors by their mechanisms of action-driven transcriptomic profiles. BMC Genomics 17, 84.
Waters, M.D., Fostel, J.M., 2004. Toxicogenomics and systems toxicology: aims and prospects. Nat. Rev. Genet. 5 (12), 936–948.
Weggler, B.A., Ly-Verdu, S., Jennerwein, M., Sippula, O., Reda, A.A., Orasche, J., Gröger, T., Jokiniemi, J., Zimmermann, R., 2016. Untargeted Identification of Wood Type-Specific Markers in Particulate Matter from Wood Combustion. Environ. Sci. Tech. 50 (18), 10073–10081.
Wegner, A., Sapcariu, S.C., Weindl, D., Hiller, K., 2013. Isotope cluster-based compound matching in gas chromatography/mass spectrometry for non-targeted metabolomics. Anal. Chem. 85 (8), 4030–4037.
Weng, M.W., Lee, H.W., Park, S.H., Hu, Y., Wang, H.T., Chen, L.C., Rom, W.N., Huang, W.C., Lepor, H., Wu, X.R., Yang, C.S., Tang, M.S., 2018. Aldehydes are the predominant forces inducing DNA damage and inhibiting DNA repair in tobacco smoke carcinogenesis. P Natl Acad Sci USA 115 (27), E6152–E6161.
Wernig, G., Chen, S.Y., Cui, L., Van Neste, C., Tsai, J.M., Kambham, N., Vogel, H., Natkunam, Y., Gilliland, D.G., Nolan, G., Weissman, I.L., 2017. Unifying mechanism for different fibrotic diseases. P Natl Acad Sci USA 114 (18), 4757–4762.
Wheeler, A.J., Gibson, M.D., MacNeill, M., Ward, T.J., Wallace, L.A., Kuchta, J., Seaboyer, M., Dabek-Zlotorzynska, E., Guernsey, J.R., Stieb, D.M., 2014. Impacts of Air Cleaners on Indoor Air Quality in Residences Impacted by Wood Smoke. Environ. Sci. Tech. 48 (20), 12157–12163.
WHO, 2012. Health effects of black carbon. World Health Organization (WHO) https://wweurowhoint/_data/assets/pdf_file/0004/162535/e96541pdf.
WHO, 2015. Residential heating with wood and coal: Health impacts and policy options in Europe and North America World Health Organization (WHO) https://appswhoint/iris/handle/10665/153671.
WHO, 2016a. Ambient air pollution: a global assessment of exposure and burden of disease. World Health Organization (WHO) http://appswhoint/iris/bitstream/10665/250141/1/9789241511353-engpdf.
WHO, 2016b. Burning Opportunity: Clean Household Energy for Health, Sustainable Development, and Wellbeing of Women and Children. World Health Organization (WHO) https://appswhoint/iris/handle/10665/204717.

Willis, B.C., Borok, Z., 2007. TGF-beta-induced EMT: mechanisms and implications for fibrotic lung disease. American J. Physiol.-Lung Cellular Mol. Physiol. 293 (3), L525–L534.
Woo, J.H., Shimoni, Y., Yang, W.S., Subramaniam, P., Iyer, A., Nicoletti, P., Rodríguez Martínez, M., López, G., Mattioli, M., Realubit, R., Karan, C., Stockwell, B.R., Bansal, M., Califano, A., 2015. Elucidating Compound Mechanism of Action by Network Perturbation Analysis. Cell 162 (2), 441–451.
Yang, S., Chen, Z., Cheng, Y., Liu, T., Lihong, Y., Pu, Y., Liang, G., 2021. Environmental toxicology wars: Organ-on-a-chip for assessing the toxicity of environmental pollutants. Environ. Pollut. 268, 115861.
Zong, D.D., Ouyang, R.Y., Li, J.H., Chen, Y., Chen, P., 2016. Notch signaling in lung diseases: focus on Notch1 and Notch3. Ther. Adv. Respir. Dis. 10 (5), 468–484.